ABSTRACT

MATA, LUIS ALEXANDER. Implementation of Self-Consolidating Concrete (SCC) for Prestressed Concrete Girders (Under the direction of Dr. P. Zia and Dr. M.L. Leming).

Self-Consolidating Concrete (SCC) was first developed in Japan almost 15 years ago, and it was not until the late 1990's that the U.S precast concrete industry applied the technology to architectural and structural building elements. This study describes the first experience of using SCC for prestressed concrete bridge girders in North Carolina.

A multiple-span bridge is currently under construction in eastern North Carolina using one hundred thirty AASHTO Type III girders, each 54.8 ft (16.7 m) long (NCDOT Project 8.1170903). Three girders from one production line of five girders were selected for evaluation. Two of the girders were cast with SCC and one with conventional concrete as the control.

The plastic and hardened properties of both the SCC and the conventional concrete were monitored and measured. The fresh properties of SCC included unit weight, air content, slump flow, Visual Stability Index (VSI), and passing ability as measured by J-ring and L-box. Hardened concrete tests on SCC and conventional concrete included compressive strength, static elastic modulus, elastic modulus based on resonance frequency ("dynamic" modulus) at different ages, along with creep and shrinkage. The prestressing force in the girders was monitored by load cells. Finally, the three girders were tested in flexure up to the design service load to determine and compare their load-deformation characteristics.

In general, two AASTHO Type III girders were successfully cast without any vibration using SCC, and exhibited virtually identical load-deflection relationships up to the design service load than that of the conventional concrete girder. SCC showed lower elastic modulus after strength adjustment, and higher creep and shrinkage than conventional concrete.

Implementation of Self-Consolidating Concrete (SCC) for Prestressed Concrete Girders

by

Luis A. Mata

A Thesis submitted to the Graduate Faculty of
North Carolina State University in partial fulfillment of the
requirements for the degree of Master of Science in Civil Engineering

Civil, Construction, and Environmental Engineering

Raleigh, North Carolina
November 2004

Approved by:

_____

Dr. David Johnston

_____

Dr. Paul Zia

_____

Dr. Michael Leming
Chair of Advisory Committee

Biography

Luis A. Mata was born in Caracas, Venezuela on August 9th, 1975. He graduated from San Ignacio de Loyola School in 1993. He received his BS in Civil Engineering, in June, 2002, from the Department of Civil Engineering at Universidad Católica Andrés Bello, Venezuela.

In January of 2002, he enrolled in graduate program in the Department of Civil, Construction, and Environmental Engineering studying Construction Engineering and Management taking classes towards his master of science degree. He worked on the project which investigated the implementation of Self-Consolidating Concrete (SCC) for prestressed concrete girders (NCDOT Project 8.1170903). This thesis is based on the data obtained from this investigation.

Acknowledgments

I wish to thank Dr. M.L. Leming and Dr. P. Zia for serving as my advisors during this project. Their patience in explaining concepts related to this research and in reading reports written by a non-native English speaker is greatly appreciated. I also wish to thank Mr. R. Nuñez for all his help and advice throughout the project and to Dr. D. Johnston for serving as a member of my committee. I would like to thank my fellow students at the Constructed Facilities Laboratory (CFL), especially to Gavin Wigth, Hazim Dwairi and David Chaparro; Mr. Jerry Atkinson, technician at the CFL, Mr. Lee Nelson, laboratory manager and Mr. Bill Dunleavy, electronics technician at CFL. I would also like to express my appreciation to the North Carolina Department of Transportation and the Federal Highway Administration, who sponsored the project on which this study is based. I am also grateful for the assistance provided by the entire staff of S&G Prestress Company, and Mr. Michael Means, PE, in the casting and testing of the experiment girders.

I would like to thank my parents Alfredo and Ane Miren Mata, my brother Alfredo, my sisters Ane Miren and María de Lourdes and all my friends for their encouragement, support and patience throughout my study.

Table of Contents

List of Tables

List of Figures

CHAPTER 1: INTRODUCTION

1.1 Background

Self-Consolidating Concrete (SCC), a relatively new category of high performance concrete, is proportioned such that the concrete freely passes around and through reinforcement, completely fills the formwork and consolidates under its own weight without segregation. The high flowability of SCC makes it possible to fill the formwork without vibration [Khayat, 1999; Khayat *et al.*, 2004].

Developed in Japan in the late 1980's [Ozawa, *et al.,* 1989], SCC has been a topic of research and development in many locations, especially in Japan and Europe [Ouchi, *et al.*, 2003]. SCC has been successfully used in numerous applications where normal concrete is difficult to place and consolidate due to reinforcement congestion and difficult access. Precast, prestressed bridge elements, such as AASHTO Type III girders, have congested reinforcement and tight dimensional geometry, and therefore can benefit from the use of SCC.

Three basic characteristics are required to obtain SCC: high deformability, restrained flowability and a high resistance to segregation [Khayat, *et al.*, 2004]. High deformability is related to the capacity of the concrete to deform and spread freely in order to fill all the space in the formwork. It is usually a function of the form, size and quantity of the aggregate, and the friction between the solid particles, which can be reduced by adding a high range water-reducing admixture (HRWR) to the mixture. Restrained flowability represents how easily the concrete can flow around obstacles, such

as reinforcement, and is related to the member geometry and the shape of the formwork. Segregation is usually related to the cohesiveness of the fresh concrete, which can be enhanced by adding a viscosity-modifying admixture (VMA) along with a HRWR, by reducing the free water content, by increasing the volume of paste, or by some combination of these factors. Two general types of SCC can be obtained: (1) concrete with a small reduction in the coarse aggregate, containing a VMA, and (2) concrete with a significant reduction in the coarse aggregate content without any VMA.

SCC has been claimed to offer many advantages for the precast, prestressed industry including elimination of noise and problems related to concrete vibration, lower labor cost per member, and faster casting, thereby increasing productivity. Due to the low water-cement ratio, SCC should have improved to durability and strength.

Generally, SCC contains a higher cementitious materials and lower water-cement ratio than conventional concrete, and so can provide relatively high strength. The paste usually includes fly ash, slag, silica fume, or other supplementary cementitious materials, or an inert filler such as limestone powder. The paste content of SCC is also relatively high, with a reduction in the size and quantity of coarse aggregate. These factors are typically associated with increased creep and shrinkage, and may be related to a reduction in elastic modulus.

1.2 Problem Statement

There are currently no universally accepted design, proportioning or acceptance criteria for the use of SCC in prestressed girders. Although SCC has been used successfully in several precast and cast-in-place applications and many of the properties of SCC have been established, several issues must still be resolved in order to successfully use SCC in the production of prestressed bridge elements. Many of these concerns are related to long term behavior of the element in service.

SCC is similar to conventional concrete in terms of compressive strength. Due to the lower content of coarse aggregate, however, there is some concern that (1) SCC may have a lower modulus of elasticity, which may affect deformation characteristics of prestressed concrete members and (2) creep and shrinkage will be higher, affecting prestress loss and long term deflection.

1.3. Objectives

There were two primary objectives of this study:

1. Compare important mechanical properties of SCC used in the production of two prestressed SCC girders to conventional concrete typically used in prestressed, precast members. These properties include compressive strength, modulus of elasticity, shrinkage and creep.
2. Compare the results of static load tests of two SCC girders and one non-SCC girder, up to full service load conditions.

The findings of this study will be useful to the precast, prestressed concrete industry by contributing to the understanding of member behavior utilizing SCC.

1.4 Methodology

A multiple-span bridge is currently under construction in eastern North Carolina using one hundred thirty AASHTO Type III girders, each 54.8 ft (16.7 m) long (NCDOT Project 8.1170903). Three of these girders, from one production line of five girders, were selected for evaluation. Two of the girders were cast with SCC and one with conventional concrete as control. The mixture proportions and placement procedures were observed and documented, and the fresh and hardened concrete characteristics were measured.

Test specimens were prepared from the concrete mixtures used in the girders. The specimens were cured along with the girders in order to determine the various properties of the SCC and compare these with similar tests of non-SCC samples. Tests on fresh SCC included unit weight, slump flow, J-Ring, air content and L-Box, while tests on fresh conventional concrete included unit weight, slump and air content tests. Hardened concrete tests on SCC and conventional concrete included compressive strength, static elastic modulus, elastic modulus based on resonance frequency ("dynamic" modulus) at different ages, along with creep and shrinkage.

The initial tension in the strand and the tension immediately before release of prestress in the girders were determined by using load cells installed with four selected strands. Load

tests of the two prestressed SCC girders and one conventional concrete girder approximately 90 days after fabrication were conducted in order to obtain the load-deformation data.

CHAPTER 2: LITERATURE REVIEW

2.1 Development of Self-Consolidating Concrete

The idea of a concrete mixture that can be compacted into every corner of a formwork, purely by means of its own weight and without the need for vibration, was first considered in 1983 in Japan, when concrete durability, constructability and productivity became a major topic of interest in the country. During this period, Japan was suffering a reduction in the number of skilled workers in the construction industry which directed affected the quality of the concrete as placed.

In order to achieve acceptable concrete structures, concrete consolidation is required to completely fill and equally distribute the mixture with minimum segregation. One solution to obtain acceptable concrete structures, independently of the quality of construction work, is the employment of Self-Consolidating Concrete (SCC). The use of SCC can reduce labor requirements and noise pollution by eliminating the need of either internal or external vibration.

Okamura proposed the use of SCC in 1986. Studies to develop SCC, including a fundamental study on the workability of concrete, were carried out by Ozawa and Maekawa at the University of Tokyo, and by 1988 the first practical prototypes of SCC were produced. By the early 1990's Japan started to develop and use SCC and, as of 2000, the amount of SCC used for prefabricated products and ready-mixed concrete in Japan was over 520,000 CY (400,000 m^3) [Ouchi *et al.* 2003].

In 1996, several European countries formed the "Rational Production and Improved Working Environment through using Self-compacting Concrete" project in order to explore the significance of published achievements in SCC and develop applications to take advantage of the potentials of SCC. Since then, SCC has been used successfully in a number of bridges, walls and tunnel linings in locations in Europe [Ouchi *et al.* 2003].

During the last three years, interest in SCC has grown in the United States, particularly within the precast industry. SCC has been used in several commercial projects [Ozyldirim, 2003; Ouchi *et al.* 2003]. Numerous research studies [Khayat *et al,* 2001; Chan *et al,* 2003; Sonebi *et al* 2003], have been conducted recently with the objective of developing raw material requirements, mixture proportions, material requirements and characteristics, and test methods necessary to routinely implement SCC.

By 2003, the Precast/Prestressed Concrete Institute (PCI), The American Concrete Institute (ACI) and the American Society for Testing and Materials (ASTM) had developed similar definitions for SCC:

> "A highly workable concrete that can flow throw densely reinforced or complex structural elements under its own weight and adequately fill voids without segregation or excessive bleeding without the need for vibration" (*Interim Guideline for the use of Self-Consolidating Concrete in the Precast/Prestressed Concrete Institute member plants, TR-6-03, Precast/Prestressed Concrete Institute*)

> "Highly flowable, non-segregating concrete that can spread into place, fill the formwork, and encapsulate the reinforcement without any mechanical consolidation"(*ACI International, Committee 237 Self-Consolidating Concrete, July 2003*).

> "Concrete that can flow around reinforcement and consolidate within formwork under its own weight without additional effort, while retaining its homogeneity" (*ASTM Sub-Committee C09.47 Self-Consolidating Concrete, December 2003*)

The latest studies of SCC focused on improved reliability and prediction of properties, production of a dense and uniform surface texture, improved durability, and both high strength and earlier strength permitting faster construction and increased productivity [Khayat *et al,* 2004; Khayat *et al,* 2001; Khayat *et al,* 2002; Chan *et al,* 2003; Sonebi *et al* 2003].

2.2 Materials for Self-Consolidating Concrete.

2.2.1 Portland Cement and Supplementary Cementitious Materials

Cementitious materials are the components that bind all of the other concrete components together. The combination of portland cement, supplementary cementitious materials and water is defined as paste, and when sand is added to the paste, mortar is formed. In order to achieve a properly proportioned SCC mixture, an increase in the paste volume is

required to achieve the required deformability. For SCC mixtures, cement contents from 650 pcy to 840 pcy (385 kg/m^3 to 500 kg/m^3) have been used with satisfactory results [Assaad et al, 2004].

The early strengths of the concrete are usually higher for those with cements with a larger amount of C_3S and C_3A and lesser amount of C_2S. Type III or high early cement, which is more finely ground and generally contains more C_3S and often more C_3A than Type I is usually used for precast operations.

Silica fume, Class F fly ash, and ground granulated blast furnace slag (GGBFS) reduce permeability and improve the chemical durability of moist cured concrete. Silica fume and Class F fly ash are pozzolanic materials, while the slag is considered a cementitious material. For precast operations, silica fume has been the most commonly used, but the use of Class F fly ash and slag has increased in recent years [Gerwick, 1993].

Pozzolanic materials do not hydrate by themselves, but only in the presence of soluble alkali and calcium products, such as calcium hydroxide, which is a by-product of portland cement hydration. The hydration rate of pozzolanic materials is slower than that of portland cement, consequently additional curing time is needed and the early heat generation is considerable reduced. Lower early strengths and higher ultimate strengths are obtained. An increase of permeability is also obtained when pozzolanic materials are used to replace portland cement. A decrease in permeability is also obtained due to the reaction with the calcium hydroxide. The reduction in early strength, which occurs when

portland cement is replaced in part by a pozzolan, is the primary reason such materials are not often used in precast operations.

Class F fly ash is a finely divided ash left after hard coal is burned for power. If cement is replaced by fly ash, the paste volume of the concrete will increase, bleeding will be decreased and , due to the increase of paste, the shrinkage will be increased. Class F fly ash is generally used to replace portland cement in the range of 15% to 25% of total cementitious material in conventional mixtures. Khayat et al [2003] reported that using 40% Class F in a SCC mixture resulted in good workability, with acceptable strength development and frost durability.

Silica-fume, also known as condensed silica fume or microsilica (ACI 116R), is a very fine, non-crystalline silica produced in electric arc furnaces as a by-product of the production of elemental silicon or silico-alloys. It is basically a “super-pozzolan” with a very high durability and excellent strength, but it is expensive and creates a high water demand, thus requiring the use of HRWR. Silica-fume is generally used in quantities of 3% to 6% of the total cementitious materials in concretes with accelerated curing.

Slag is a by-product of the iron industry, generally used to replace portland cement in the range of 40% to 60% of total cementitious material in conventional concrete mixtures. Lachemi et al. [2003] obtained effective results incorporating 50% to 70% slag as cement replacement with different Viscosity Modifier Admixtures (VMA) for various SCC mixtures. Mixtures containing slag as a partial replacement of portland cement generally

have lower early strengths and higher ultimate strengths than otherwise comparable mixtures containing only portland cement.

The addition of a supplementary cementitious material will not reduce early strengths. These materials can therefore be used to enhance both deformability and durability without sacrificing early strength. Supplementary cementitious materials may not be available at precast facilities, however, and so SCC mixtures in precast operations must often be based on portland cement only. Otherwise, the operation will have to expend considerable capital to modify storage and batching equipment.

2.2.2 Aggregates

The development and use of SCC have shown that it can be successfully produced using a broad range of materials but it is often difficult to predict the resulting properties of the concrete without trial batches. Okamura [1997] reported that if the coarse aggregate content of a SCC concrete mixture exceeds a certain limit, blockage would occur independently of the viscosity of the mortar. Superplasticizer and water content are then determined to ensure desired self-consolidating characteristics. Yugi et al [1993] reported that reducing the volume of coarse aggregate in a SCC mixture is more effective than decreasing the sand-to-paste ratio to increase the passing ability through congested reinforcement.

The size, shape and, to a certain extent, the gradation of the aggregate in an SCC mixture are important to minimize the collision and contact between the solid particles near an

opening, which is directly related to the concrete passing ability. Bui *et al*., [2002] proposed a rheological model for SCC relating the rheology of the paste to the average aggregate spacing D_{SS} and average aggregate diameter D_{av} to consider the effect of most of the factors related to aggregate properties and content. Bui and others reported that a higher aggregate spacing requires a lower flow and higher viscosity of the paste to achieve satisfactory deformability and segregation resistance of SCC. Better results were also obtained with the same spacing and a smaller aggregate diameter.

For most prestressed concrete products, the maximum size of the coarse aggregate does not exceed ¾ in (20 mm) and is often limited to ½ in (12 mm) or 3/8 in (9.5 mm) due to reinforcement spacing. The coarse aggregate should not contain clay seams that may produce excessive creep and shrinkage. The aggregates must be clean and of a proper temperature for incorporation in the mix [Gerwick, 1993]. For SCC mixtures, a coarse aggregate size of 0.2 to 0.55 in (5 mm to 14 mm) and quantities varying from 1,335 pcy to 1454 pcy (790 kg/m^3 to 860 kg/m^3) have been used with satisfactory results [Khayat, *et al*, 2004].

2.2.3 Water Reducing Agents (WRA) and High Range Water Reducers (HRWR)

Water reducing agents (WRA) and high range water reducers (HRWR) are surfactants that promote dispersion of cement particles (ACI 212.4R-93). The main difference regarding performance between these two "lubricants" is that the HRWR's are three to four times more effective in increasing the fluidity of the system than WRA's; they are also more expensive than WRA. The use of a HRWR for the achievement of SCC is

indispensable [Okamura, *et al.*, 1996]; they can increase paste flowability with a slight decrease of viscosity [Khayat, 1999].

2.3 Characteristics of Fresh Self-Consolidating Concrete

Previous studies [Khayat, *et al*, 2004; Kaszynska, *et al*, 2003] report that SCC should be produced to meet three basic characteristics: high deformability, high passing ability and high resistance to segregation. Deformability of concrete is defined as the ability of the concrete to undergo a change in shape under its own weight. High deformability is required so that the concrete can spread uniformly into the formwork.

In order to obtain adequate deformability, it is important to minimize the friction between the solid particles of the mixture. Reduction of the coarse aggregate and an increase in the paste volume is required to achieve the desired deformability [Khayat, *et al*, 2004]. Another way to reduce inter-particle friction is with the incorporation of continuously graded fillers, such as limestone filler, and by minimizing use of gap-graded or uniformly-graded aggregates.

The deformability of the concrete is directly related to the deformability of the paste. To increase the deformability of the paste and reduce the internal friction of solid particles, a High Range Water Reducing Admixture (HRWR) is commonly used in SCC mixtures. A HRWR can be used to maintain a relatively low water cementitious materials ratio (w/cm) while increasing fluidity. The deformability of the paste is increased by reducing

the viscosity. A highly flowable concrete can be obtained without a significant reduction in cohesiveness, improving the resistance to segregation [Khayat, *et al*, 2004].

Blockage is caused by the collision and contact between the solid particles near an opening, therefore the size and the coarse aggregate content in a SCC mixture is directly related to the concrete passing ability. High passing ability is needed to achieve SCC. The passing ability requirements depend on the formwork geometry and the extent of congestion of the reinforcement. Providing adequate viscosity to the mixture reduces the risk of blockage. If a SCC mixture is highly deformable, but has insufficient cohesiveness, the concrete may not distribute itself uniformly throughout the formwork. A mixture with low deformability can result in segregation which can also lead to blockage when the concrete attempts to pass the reinforcement.

The third property of SCC is to have sufficiently high resistance to segregation to ensure a homogenous distribution within the form. Adequate cohesiveness can be obtained by incorporating a viscosity-modifying admixture (VMA) along with HRWR to control bleeding, segregation, and surface settlement [Khayat, *et al*, 1997]. Another approach to secure adequate cohesiveness is to reduce the free water content and to increase the volume of sand and cement paste. Supplementary cementitious materials and fillers with a large surface area can adsorb considerable more water than the same mass of cement particles, reducing the free water content of the mixture [Miura, *et al*, Trudel, 1996]. Non-compatibility problems between the cement and superplasticizer may be more critical with SCC than conventional mixtures [Kaszynska and Nowak, 2003].

2.4 Use of Self-Consolidating Concrete in Precast/Prestress Products

The use of SCC in precast/prestress applications has progressed faster than in cast-in-place structures due to several reasons. Fabrication of precast/prestress members takes place in a more controlled environment with less variation in mixtures and activities than cast-in-place construction. Less variation in production due to a relatively lower change in member variety permits more consistent in-plant operations. Unit costs are easier to track and control. Although virtually all commercial concrete contains chemicals admixtures, the use of chemical admixtures and low water cement ratio commonly used in precast/prestress mixtures can make transition to SCC easier than in ready-mixed concrete production [Schlagbaum, 2003]. Greater engineering scrutiny due to DOT requirements for precast, prestress operations directly affects quality control and quality assurance of the concrete. High early strength with low w/c is typically more critical in precast/prestress [Garwick, 2003], which can improve durability.

2.5 Economic Impact of Self-Consolidating Concrete in Precast Applications

The economic impact of SCC in precast/prestress applications can be assessed in three categories: concrete mixture proportions and raw materials, production costs, and finished product improvements.

Due to the larger quantities of portland cement or supplementary cementitious materials used in SCC, the cost of the raw materials is usually greater. Cementitious material may be required more to increase the fines content to achieve stability that is needed on the

basis of strength alone. In addition to cement, the cost of admixtures, such as HRWR and possibly a Viscosity Modified Admixture (VMA), will also increase the cost of SCC. Many precast concrete producers have switched from more angular coarse aggregates to more rounded aggregates. Typically, precast concrete producers will pay an additional 8-12% on average for raw materials in a SCC mixture relative to the raw materials cost of traditional concrete mixtures [Martin, 2002].

Chemical admixtures can increase the cost of the SCC mixture, but are necessary to achieve the desired concrete properties. Such is the case with VMAs which are added to improve the stability and help prevent segregation during placement. The extra cost would be around 2% of the cost of the mixture, but can yield savings by minimizing the need to increase the cement content in the SCC mixture, allow a broader variety of aggregates to be used and minimize the impact of moisture content in the aggregates [Martin, 2002].

The SCC mixture cost can also be reduced by the use of pozzolanic materials such as fly ash, which is typically one-third to one-half the cost of cement. Fly ash can also help improve the flowability and stability of the SCC mixture [Lachemi, *et al., 2003*].

The extra cost of the SCC mixture is compensated by production cost efficiencies such as reduction in placing time, vibrator use and maintenance, form maintenance, and improvement worker safety. Placing time is the time it takes to transfer the concrete from the transportation unit to the form and consolidate it. Improved productivity by reducing

time, labor or equipment may easily compensate for additional material costs. A case study for tracking the time required for placing double-tee beds in a precast plant reported a reduction of 20% compared to a conventional mixture, with a 32% reduction of labor involved in the process [Martin, 2002]. Regardless of the applications, an average reduction in labor during the placing process is estimated to be about 30% using SCC [Schlagbaum, 2002].

The service life of vibration equipment and forms will increase with the use of SCC. A reduction in vibration operations will not only reduce maintenance and investment cost, but also improves the operating conditions at the plant by reducing noise levels. Reducing the exposure of workers and eliminating requirements for hearing protection may reduce insurance and safety costs. Due to the elimination of vibration to consolidate the mixtures, the forms use in the precast operations will receive less wear and tear, decreasing the regular maintenance costs and the costs of investing in new forms.

Patching operations and finished product improvements may be critical for certain precast concrete producers, especially for architectural panels. Properly proportioned SCC has been proven to reduce the number of "bugholes," honeycombing and other surface imperfection on the finished concrete surface [Martin, 2002]. Jansen [2002] and others however, have noted that poorly proportioned SCC can result in significant segregation and very poor surface finish.

Bugholes are small imperfections located on the surface created by air trapped between the form and the concrete. Effective vibration can minimize the amount of bugholes, but never eliminate them entirely. Bugholes are also affected by admixtures and release agents. With a properly proportioned SCC mixture, the concrete can freely fill all the spaces of the form under its own weight minimizing or even eliminate the trapped air. A key economic factor for using SCC in prestressed girders is the finishing of the product. Several state transportation agencies, such as NCDOT, require all the products to have a smooth finish with minimal bugholes for both sides of the girders.

If the quantity and size of bugholes can be minimized, the amount of work and cost related to finishing the girders will be significantly reduced. Finishing and retouching of the girders can represent a significant part of labor costs in the precast concrete operations. S&G Prestress, a prestressed concrete producer located in North Carolina, estimates that the amount of labor required to patch bugholes may be reduced by half [Means, 2004].

Honeycombing is an imperfection caused by insufficient or inadequate vibration. Although the occurrence of honeycombing is relatively low in a well controlled precast plant, it also represents an increase in the cost due to retouching and finishing. Honeycombing can be reduced with a properly proportioned SCC mixture.

The use of SCC can reduce patching expenses and manpower needed for patching finished precast elements. In many examples of structural, architectural, and utility

products, producers in the United States have reported a decreased patching labor cost from 25-75% [Martin, 2002].

2.6 Testing Fresh Self-Consolidating Concrete

ASTM Committee C09.47 on Concrete and Concrete Aggregates formally undertook the task to develop the procedures to test SCC on June 2001 [Vachon, 2002]. Although several tests have been developed to evaluate the performance of a fresh SCC, only the Slump Flow test and the J-Ring test are widely used for acceptance testing. These tests are under development as standard test methods by ASTM.

Other test methods, which are more often used in developing SCC mixtures, are the L-box and column test. These tests, also in development by ASTM, are used to test the passability of the mixture and the tendency to segregation.

The conventional slump test is used to provide a measure of the plasticity of the fresh concrete. The Slump Flow test provides a measure of flowability. The test consists of measuring the mean diameter of the spread of the fresh concrete after flowing from an inverted slump cone (Figure 2.1). The test determines the capacity of the SCC to deform under its own weight. The time the sample takes to spread 20 in (500 mm), is also often used to characterize flowability.

(a)

(b)

Figure 2.1 Slump flow test for SCC. a) concrete after flowing from an inverted slump cone. b) Measurement of the spread concrete at the end of the flow.

A sample of freshly mixed concrete is placed in an inverted slump cone; the concrete is placed in one lift and not consolidated by any means of mechanical agitation. The inverted slump cone is raised, and the concrete allowed to flow out and spread without hindrance. The diameter of the spread concrete at the end of the flow is measured across. The diameter is also measured at an angle perpendicular to the original measured diameter. If the measurement of the two diameters differs by more than 2 in (50 mm), the test is invalid and shall be repeated. The average spread is reported to the nearest half inch. Values from 24 to 19 in (600 to 730 mm) are considered acceptable [Khayat et al, 2004]. A minimum value of 20 in (560 mm) is required for classification as SCC.

The J-ring Test is used to assess the passing ability of the concrete [Bartos, 1998]. The J-ring is a 1 in wide and by ½ in thick metal ring with a central diameter of 12 in with 16 separated 5/8 in bars, spaced evenly around the ring (Fig 2.2 and 2.3). The ring is used in conjunction with a slump cone. A sample of freshly mixed SCC is placed in the inverted slump cone which is placed concentrically in the J-ring. The concrete is placed in one lift and not consolidated. The cone is raised and the concrete allowed to spread, passing through the J-Ring bars. The mean diameter of the spread concrete is determined as for the Slump Flow test.

(a)

(b)

Figure 2.2 J-Ring test for SCC. a) Filling the inverted slump cone. b) Concrete spreading through J-Ring rods.

Figure 2.3 Measurement of the concrete spread.

Figure 2.4 L-Box apparatus

The J-ring is commonly used in conjunction with the slump flow to measure the passing ability of SCC, that is, the ease with which the concrete passes through reinforcing bars. Brameshuber, *et al*, (2001) proposed that the difference between the flow test and the J-ring test not to exceed 2 inches (50 mm) in order for the mixture to pass through the reinforcement successfully. In 2002, the European Federation for Specialist Construction Chemicals and Concrete Systems (EFNARC) changed this value to 0.4 inches (10 mm) [Bartos, 1998; Khayat, *et al*, 2004].

The L-box test is an alternate passing ability test. This test simulates the casting process by forcing the concrete to flow through reinforced bars under a static pressure. The L-box is an L-shaped device as shown in Figure 2.4. The height of the concrete at the end of the test at the vertical section and the end of the device is h_1 and h_2 respectively. The vertical section of the device is filled with 0.4 ft^3 (12 liters) concrete and allowed to rest for a minute. The gate that separates the two sections is then lifted and the concrete flows through the reinforcing bars. The height of the concrete in the vertical section (h_1=600-H_1) and the height of the concrete at the end of the device (h_2=150-H_2) are measured. The self-leveling characteristic of the concrete is evaluated by using the ratio h_2/h_1 [Khayat, *et al*, 2004]. The acceptable limit proposed by Skarendahl (1999) for blocking and segregation should be between 0.80 and 0.85. EFNARC guidelines establish the limit to be between 0.8 and 1.0 [Khayat, *et al*, 2004].

2.7 Mechanical Properties of Self-consolidating Concrete

The mechanical properties and behavior of SCC are similar to conventional concrete in terms of compressive strength. There is some concern that SCC may have a lower modulus of elasticity due to lower coarse aggregate content, which may affect deformation characteristics of prestressed concrete members. Additionally, creep and shrinkage are expected to be higher for SCC due to its high paste content, affecting prestress loss and long term deflection, although this may be offset in part due to relatively low w/c of SCC commonly used in precast operations.

2.7.1 Modulus of Elasticity

The static modulus of elasticity of a material under tension or compression is given by the slope of the stress (σ) – strain (ε) curve under uniaxial loading. Three methods for calculating the modulus are used for concrete as shown in Figure 2.5 [Mehta, 1993]:

1.- The initial tangent modulus is given by the slope of a line drawn tangent to the stress-strain curve at any point of the curve. It is approximately equal to dynamic (low strain) modulus.

2.- The secant modulus is given by the slope of a line drawn tangent from the origin to the point on the curve corresponding to the 40% stress level of the failure load.

3.- The chord modulus is given by the slope of a line drawn between two points of the stress-strain curve. Compared to the secant modulus, instead of the origin the line is drawn from a point representing a longitudinal strain of 50 microstrain to the point that corresponds to 40% of the ultimate load.

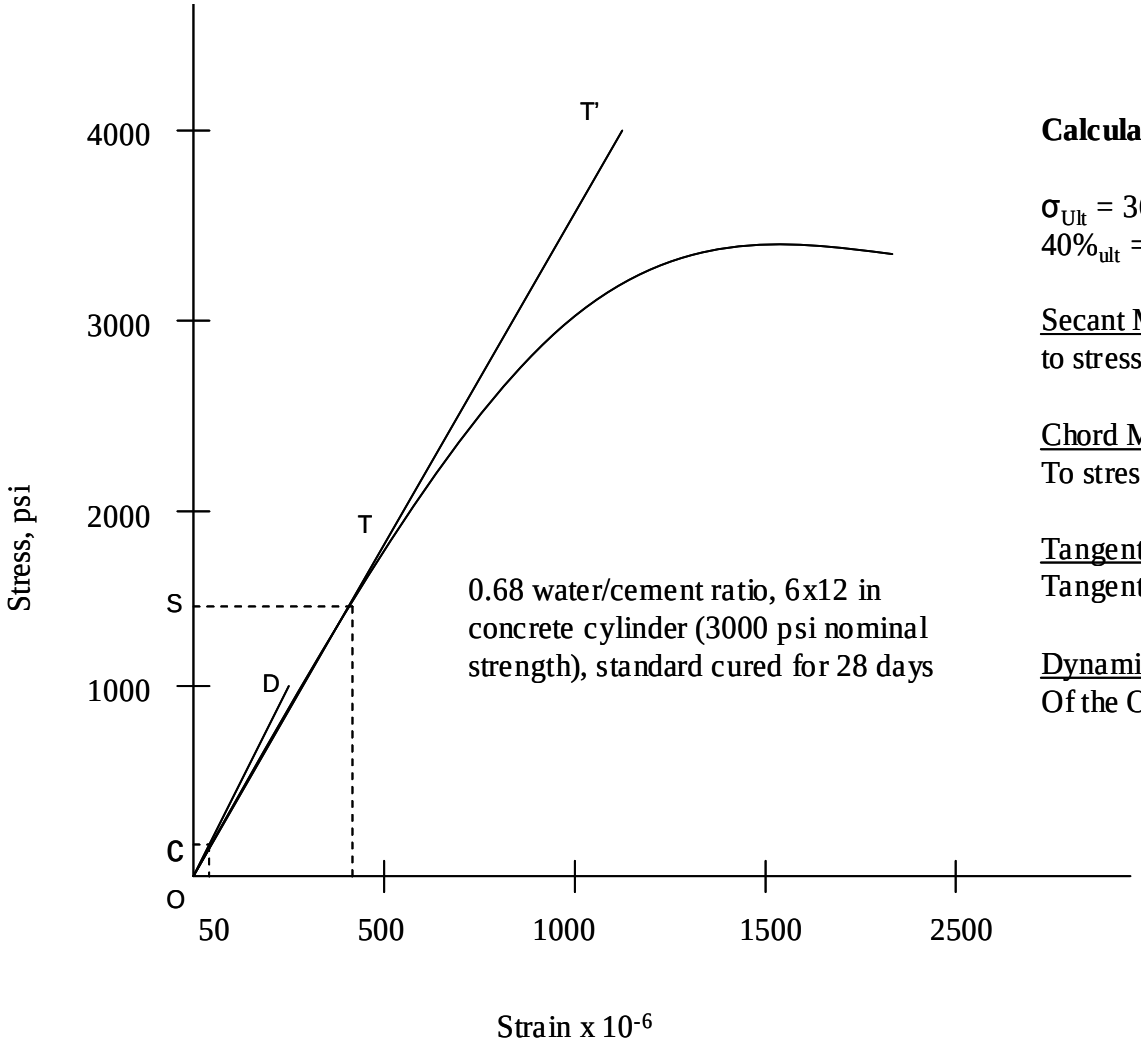

Calculating the elastic modulus

σ_{Ult} = 3600 psi
$40\%_{ult}$ = 1440 psi = S0

Secant Modulus: Slope of the line corresponding to stress SO=1440/400= 3.6 Mpsi

Chord Modulus: Slope of the line corresponding To stress SC=(1440-200)/(400-50)=3.5 Mpsi

Tangent Modulus: Slope of the line TT^1 drawn Tangent to any point on the σ-ε curve

Dynamic Modulus (Initial tangent modulus): Slope Of the OD from the origin=1000/200=5 Mpsi

Fig 2.5 Example of the different types of elastic modulus and the method by which these are determined [Mehta, 1993]

The ratio of the static modulus of elasticity to the dynamic modulus is always less than one [Neville, 1996]. The dynamic modulus of elasticity is generally around 20 percent higher than the static modulus of elasticity for high, medium and low strength concretes respectively [Mehta, 1993].

Modulus of elasticity can be computed as

$$E = \frac{s}{e} \tag{2.1}$$

where:

σ = Stress

ε = Strain

The Prescast/Prestressed Concrete Institute (PCI) Design Handbook uses the equation given in ACI 318-95 to estimate elastic modulus (E_c). ACI 318-02 permits this equation for concrete with a unit weight between 90 and 155 lb/ft^3.

$$E_c = w^{1.5} 33 \sqrt{f'_c} \tag{2.1}$$

where:

E_c = modulus of elasticity of concrete, psi

w = unit weight of concrete, pcf

f'_c = compressive strength

For normal weight concrete, E_c may be estimated more simply as:

$$E_c = 57{,}000 \sqrt{f'_c} \tag{2.2}$$

For concrete compressive strengths greater than 6000 psi, Eq 2.2 may predict an unrealistically high estimate of E_c. For higher strength concrete ACI 363R-92 estimates E_c as:

$$E = 40{,}000\sqrt{f'_c} + 10^6 \tag{2.3}$$

Equation 2.3 is still under revision due to the small aggregate size and high paste content used to establish his relation.

The modulus of elasticity of concrete is affected by the elastic modulus of the aggregate and by the volumetric proportion of aggregate in the concrete, the elastic modulus of the cement paste and, to a certain extent, the method of measurement. The elastic modulus of the cement paste matrix is affected by the strength and therefore the w/c and extent of curing. Due to the higher paste content and lower content of coarse aggregates in SCC mixes, E_c is expected to be lower for SCC than conventional concrete. For the same compressive strength, the dynamic modulus of SCC compositions was found to be lower than for conventional concrete [Turcry, ***et al.***, 2003].

Determination of the static modulus of elasticity (E_c) procedure using concrete samples is described in ASTM C469. The dynamic elastic (Young's) modulus can be determined non-destructively on concrete disks using resonant frequency principles similar to those found in ASTM C 215 "Standard Test Method for fundamental Transverse, Longitudinal, and Torsional Frequencies of Concrete Specimens" [ASTM 2002] adapted for thin circular specimens. A method of determining the dynamic elastic modulus of circular concrete disk

based on resonant frequency is discussed in detail by Leming, Nau and Fukuda [1998]. A short overview of the method is provided here.

Determination of the dynamic elastic modulus of a disk is based on the theory developed by Hutchinson (1979) assuming axisymmetric flexural vibration of a thick, free, circular plate, including shear and rotary inertia effects. Dynamic elastic modulus of a disk under free-free vibration is

$$E_d = 2(1+n)r\left(\frac{pfd}{\Omega_0}\right) \tag{2.4}$$

where

E_d = dynamic elastic modulus

v = Poisson's ratio

ρ = the mass density of the disk

f = the fundamental cyclic natural frequency in Hertz

d = the diameter of the disk

Ω_0 = the frequency parameter associated with the fundamental vibration mode

E_d may be determined by measuring f, d and ρ, estimating v, and obtaining Ω_0 from an iterative solution, which is implemented using a spreadsheet or other software with Bessel function and matrix mathematical capabilities.

2.7.2 Creep and Shrinkage

The stress and strain at any section of a prestressed concrete structure change gradually over time, due to creep and shrinkage of concrete, and relaxation of the steel. Whenever a stress is

applied to concrete, a strain in the material is produced and it will progressively increasing over time as long as the stress is sustained. This elastic shortening is due to creep which, in prestressed concrete members, can lead to a substantial loss of prestress.

Plastic shrinkage is caused by drying of the surface relative to the rate of evaporation, which is affected by humidity, wind temperature and velocity, and the rate of bleeding. Plastic shrinkage of SCC compositions can be at least four times higher than ordinary concrete as reported by Turcry, *et al* [2003], with SCC plastic shrinkage was about 1,000 microstrain higher than conventional concrete.

Drying shrinkage is caused by the loss of moisture in the capillary pores. The loss of adsorbed water causes changes in the microstructure of the concrete, causing both irreversible and reversible volume changes. Drying shrinkage occurs over long periods of time and is related to the characteristics of the paste, including water content, water cement ratio, pore size distribution, and the volume of the paste. Drying shrinkage is also affected by the aggregate, primarily as a function of the volume and to certain extent as a function of the stiffness of the aggregate. Powers [1961] found that the ratio of shrinkage of concrete (S_c) to shrinkage of the cement paste (S_p) can be related exponentially to the volume fraction of the aggregate (g) in concrete

$$\frac{S_c}{S_p} = (1-g)^n \tag{2.5}$$

L'Hermite [1962] found that the values of *n* varied between 1.2 and 1.7 depending on the elastic modulus of the aggregate; a value of 1.5 is commonly used.

An average value of $(\varepsilon_{SH})_u$ is recommended by ACI Committee 209 (1992) as 800 and 730 microstrains for moist cured for 7 days and steam cured for 1-3 days respectively, with a value of 780 microstrains for both moist and steam cured. For standard conditions, the Prestressed Concrete Institute stipulates an average value of 820 microstrains for ultimate shrinkage.

Drying shrinkage and creep are commonly studied together due to several reasons: 1) both originate from the hydrated cement paste, 2) strain-time curves are very similar, 3) both are generally influenced by same factors, 4) the microstrain of each cannot be ignored in structural design and 5) both are partially reversible [Mehta, 1993]. Shrinkage and creep occur together in practice and each influences the other.

Because of the higher paste content and lower content and size of coarse aggregates in SCC mixes, drying shrinkage is generally assumed to be higher for SCC than conventional concrete. Drying shrinkage of SCC may be as 25% higher than that of normal concrete [Raghavan, *et al*, 2003].

Creep is affected in much the same way by the same factors that affect drying shrinkage. It is also related to movement of moisture, but the driving factor is an external load rather than different humidities. The deformation resulting from this time-dependant behavior is a function of the age of loading, the magnitude and duration of the applied load, concrete properties, curing and environmental conditions. ACI Committee 209 (1992) proposes a format for creep similar to that for shrinkage; the expression for creep is:

$$C_t = \frac{t^a}{a + t^a} C_u \tag{2.6}$$

where a and α are experimental constants and t, in days, is the duration of loading. For standard conditions, ultimate shrinkage strain for a conventional concrete using granite as the coarse aggregate is around 900 microstrains [Neville, 1998].

Branson (1971, 1977) formed the basics for equations 2.6 and 2.7 in a simplify creep evaluation. The additional strain ε_{cu} due to creep can be defined as

$$e_{cu} = r_u f_{ci} \tag{2.7}$$

where

ρ_u = unit creep coefficient, generally called specific creep

f_{ci} = stress intensity in the structural member corresponding to initial unit strain ε_{ci}

Due to the linear stress-strain relationship of creep, it is feasible to relate the creep strain ε_{CR} to the elastic strain $\varepsilon_{EL.}$ A creep coefficient C_u can be defined as

$$C_u = \frac{e_{CR}}{e_{EL}} = r_u f_{ci} \tag{2.8}$$

Therefore, the creep coefficient at any time t in days can be defined as

$$C_t = \frac{t^{0.60}}{10 + t^{0.60}} C_u \tag{2.9}$$

Raghavan, *et al.* [2003] reported that SCC shows a greater initial elastic deformation, but the permanent strain induced by creep in SCC is lower compared to normal concrete. Raghavan, *et al*, [2003] also reported that the rate of creep was reduced by 33% for normal concrete and 50% for SCC between 7 and 28 days.

2.7.3 Permeability

Permeability is defined as the ease with which fluids, both liquids and gases can enter into or move through the concrete. The ease with which air or other gases penetrate into concrete is related to the water permeability and therefore the durability of concrete. Air permeability is greatly affected by moisture in the concrete, cementitious materials, extent of curing and moisture of the concrete [Hearn, *et al*, 1994; Neville, 1998]. Schonlin and Hilsdorf [1998] reported that concrete made with higher w/cm shows a higher permeability index for the same duration of curing and the same curing temperature. The relation becomes smaller for longer duration of curing. Air permeability tests are very sensitive to moisture content of the sample. A wetter sample will have lower air permeability due to the water blocking the pores of the concrete and increases the time for the passage of air [Guth, 1998].

Although there is no single, standard method for air permeability, the method described by Schonlin and Hilsdorf [1998] is reasonably well known. In the Scholin and Hilsdorf method, a chamber is placed on top of a concrete disk, the air is evacuated from the chamber and the time for a given pressure change inside the chamber is determined. An equation for an air permeability index can be developed on the basis of Boyle-Marriote's law. This equation assumes a constant flow of gas and treats the concrete as a homogeneous porous material.

$$API = \frac{(P_1 - P_0)V_s L}{(t_1 - t_0)A\left[p_a - \frac{P_1 + P_0}{2}\right]} \tag{2.9}$$

where:

API = permeability index ($\mu m^2/s$ or in^2/s)

P_0 = pressure inside the chamber at start of experiment (mm-Hg or in-Hg)

P_1 = pressure inside the chamber at end of the experiment (mm-Hg or in-Hg)

p_a = atmospheric pressure (mm-Hg or in-Hg)

V_s = volume of vacuum chamber (mm^3 or in^3)

L = Thickness of the specimen (m or in)

A = cross section of the specimen (m^2 or in^2)

t_1-t_0 = duration of test

Guth [1998] found air permeability index values of 1.72 $\mu m^2/s$ (2.67×10^{-3} in^2/s) for an ordinary portland cement concrete (w/cm = 0.44) and 0.38×10^{-3} in^2/s (0.25 $\mu m^2/s$) for an ordinary portland cement concrete (w/cm = 0.35) at 90 days. Dilek, Guth and Leming [1998] reported an air permeability index value of 0.37 $\mu m^2/s$ (0.57×10^{-3} in^2/s) for a 0.30 w/cm concrete, and an air permeability index value of 1.18 $\mu m^2/s$ (1.83×10^{-3} in^2/s) for a 0.54 w/cm concrete. Savas [2000] reported an air permeability index of 0.13×10^{-3} in^2/s (0.081 $\mu m^2/s$) and 0.04×10^{-3} in^2/s (0.028 $\mu m^2/s$) for accelerated and standard curing respectively, of low w/c mixtures at an age of 90 days (w/cm = 0.32). Differences in API for low w/c ratio concretes are normally small; high values and large differences are typically associated with microcracking.

2.8 Camber Measurement on Prestressed Girders

Prestressed concrete beams are more slender than reinforced concrete beams due to the high span/depth ratio; therefore deflection is more important in design. For prestressed girders, camber may be important. Camber may increase with concrete creep and time, and bridge camber may make the pavement uneven and even dangerous.

The PCI design handbook [1991] gives expressions for determining the upward deflection that results from the prestressing force. The equation given to calculate the initial camber for a girder with straight strands is as follows:

$$\Delta = \frac{P_i e l^2}{8EI} \uparrow \tag{2.10}$$

where:

Δ = deflection caused by prestress force

P_i = initial prestress force

e = eccentricity

l = length of the girder

$E = E_{ci}$ = modulus of elasticity at release

I = moment of inertia of the section

Equation 2.10 does not take into account the weight of the girder itself, which is given in Equation 2.11.

$$\Delta = \frac{5wl^4}{384EI} \downarrow \tag{2.11}$$

where:

w = weight of the concrete per unit length

l = length of the girder

$E = E_{ci}$ = modulus of elasticity at release

I = moment of inertia

The initial camber at the time of prestress release can be predicted by subtracting the downward deflection from the upward deflection as shown on Equation 2.12.

$$\Delta_{Total} = \frac{P_i e l^2}{8EI} \uparrow - \frac{5wl^4}{384EI} \downarrow \tag{2.12}$$

CHAPTER 3: RESEARCH METHODOLOGY

3.1 General

In this chapter the materials used in the study, the development of test parameters and concrete mixtures and an overview of the test program are explained. Mixing procedures, preparation and curing of the specimens and the test methodologies are also reviewed.

This study examined selected concrete properties used in the production of two prestressed SCC girders and one non-SCC girder cast in the same precast, prestressed production facility. The placement procedures were observed and documented, the material characteristics were measured, and load deflection curves for the girders were measured and analyzed.

Test specimens were prepared from the SCC and control concrete used in the girders. Both girders and specimens were cured without using heat. Various properties of the SCC were compared with similar properties of non-SCC samples.

The prestress girders using the SCC mixtures were fabricated at S&G Prestress, Wilmington, North Carolina. The length of the girders and the size of the casting bed allowed casting five AASHTO Type III girders. Three of these girders were fabricated using conventional concrete, typical of that used locally in prestressed elements, while the two remaining girders were fabricated with two different batches of SSC.

The conventional concrete girders were vibrated as required by NCDOT specifications but no vibration was provided for the SCC girders. The girders were cured without using heat, and

were covered with heavy-duty tarpaulins with a soaker hose along the top of the girders to provide moisture approximately one hour after the casting. Forms were stripped approximately 18 hours after casting. For hardened concrete, tests on SCC and conventional concrete included compressive strength, static elastic modulus, elastic modulus based on resonance frequency ("dynamic" modulus), creep and shrinkage. Tests on fresh SCC included unit weight, slump flow, J-Ring test, air content, and L-Box test, while tests on fresh conventional concrete included unit weight, slump and air content. The test matrix is shown in Table 3.1. The internal temperature of the girders at various locations and the prestressing force before release were also determined. At an age of 98 days, load deflection tests in the girders were conducted.

3.2 Overview of the Test Program

Compressive strength and elastic modulus were determined to examine any differences in between conventional concrete and SCC at similar strengths after similar curing. Limited creep and shrinkage testing were included in this study to determine if the volume stability characteristics of SCC are significantly different from those of conventional concrete. The data obtained in this study should be useful for the design of prestressed members.

Segregation is one of the main concerns when SCC is used. Qualitative assessment of potential segregation was based on visual evaluation on fresh SCC using the Slump Flow, J-ring, and L-box tests. In addition in this study, the dynamic elastic (Young's) modulus was determined on disks sawn from the top, middle and bottom of 4 x 8 in cylinder samples taken from the three and different mixtures. This was done to first identify the presence of any

Table 3.1 Test Matrix for the Study

Test	Time/Condition	Test Standard	Specimen Type	Mixture		
				Non SCC	**SCC1**	**SCC2**
Fresh Concrete						
Unit weight	ASTM C 172	ASTM C 138	fresh concrete	yes	yes	yes
Slump	ASTM C 172	ASTM C 143	fresh concrete	yes		
Air content	ASTM C 172	ASTM C 173	fresh concrete	yes	yes	yes
Slump Flow	ASTM C 172		fresh concrete		yes	yes
J-Ring	ASTM C 172		fresh concrete		yes	yes
L-box	ASTM C 172		fresh concrete		yes	yes
Hardened Concrete						
f_c'	7 day	ASTM C 39	4 x 8 cylinders	2	2	2
	28 day			2	2	2
	90 day			2	2	2
E_c	7 day	ASTM C 469	4 x 8 cylinders	2	2	2
	28 day			2	2	2
	50 day			2	2	2
	60 day			2	2	2
	90 day			2	2	2
E_d	28 day		4 x1 Disks	3	3	3
	28 day		4 x 1 Diaks (sawn)	6	6	6
Creep	Load (7 day) 40% strength @ 7 days	ASTM C 512	4 x 8 cylinders	3	3	3
Shrinkage and difference of volume	Companion specimens (creep)	ASTM C 512	4 x 8 cylinders	2	2	2
	Ambient	ASTM C 157	4 x 4 x 11 prisms	2	2	2
Modulus of Rupture	28 day	ASTM C 78	6x6x20 beams	2	2	2

gradient in mechanical properties second to examine the relationship between results of tests of fresh SCC and potential segregation in the specimens. Since an increase in the quantity of coarse aggregate will typically result in higher dynamic elastic modulus, at least for conventional density and strength concrete, any tendency to segregate would result in a gradient in both mass and elastic modulus within a cylinder. SCC was placed in the cylinder without external consolidation; conventional concrete was consolidated in accordance with ASTM C-31 (AASHTO T-23).

Pretensioning jacks used during the fabrication of the girders indicates only the force at the live end of the casting bed but not for the dead end. The force at the dead end usually is not the same as that of the live end due to strand relaxation, friction, slip, and temperature variations. Measurement of the force at the dead end was recorded. Internal temperatures at various points in the girder were also determined.

3.3 Concrete Mixtures

As summarized in Table 3.2 the standard, control mixture and the SCC mixture had cement contents of 680 lbs and 810 lbs respectively, which represent an increment of 16% of cement for the SCC. A smaller aggregate content and aggregate size, # 78 (½ in to No 4), was used for the SCC mixture. The conventional concrete contained a larger quantity of a larger sized aggregate (# 67 – ¾ in to No 4). The fine aggregate was a manufactured sand conforming to the NCDOT 2MS specification. This sand was produced by crushing a local marine marl (limestone).

Table 3.2 Mixture Proportions of Conventional Concrete and SCC

Materials	**Conventional Concrete**	**SCC**
Cement (Type III), lbs	680	810
C. Aggregate – Granite, lbs, size	1,700 (#67)	1,330 (#78)
F. Aggregate - 2MS*, lbs	1,295	1,300
Water, lbs	283.6	341.9
W/C	0.42	0.42
AEA - Darex II, oz/cwt	0.3	0.3
Retarder - Daratard 17 oz/cwt	4.0	4.0
HRWR - ADVA Flow oz/cwt	5.0	n/a
HRWR - ADVA 170 oz/cwt	n/a	10.0

3.3.1 Chemical Admixtures

The chemical admixtures used in the girders were provided by Grace Construction Products. Chemical admixtures included a separate type of high range water reducer (HRWR) for the SCC and conventional concrete, an air-entraining admixture, a corrosion inhibitor and initial set retarding admixture. The addition of chemical admixtures was supervised by two Grace representatives at the time of mixing and casting the girders.

ADVA 170 and ADVA Flow conform to "Specifications for Chemical Admixtures for Concrete", ASTM C494 as a Type F admixture. The addition rates for the HRWR's may vary with the type of application, but will normally range from 3 to 9 fl oz/cwt (195 to 590 mL/100) kg of cement. The HRWR should be added with the initial mixing water. ADVA 170 is compatible with Type D water reducers as long as they are separately added to the concrete. Both ADVA 170 and ADVA Flow are third generation HRWR's.

Darex II AEA is an air-entrained admixture that meets the requirements of ASTM C260, "Standard Specification for Aid-Entraining Admixture for Concrete" [ASTM 1999] added to provide suitable air void parameters for resistance against frost attack.

Daratard 17 is an aqueous solution of hydroxylated organic compounds that retards the initial and final set of concrete. The usual addition rate of 3fl oz/cwt (195 mL/100 kg) of cement will extend the initial setting time of portland cement concrete by 2 to 3 hours at 21°C (70°). Daratard 17 meets the requirements of ASTM C494 type B and type D "Standard Specifications for Chemical Admixtures for Concrete" [ASTM 1999].

3.4 Fabrication and Curing of Specimens

All specimens were made while the girders were being cast at the prestressing plant. Concrete samples for conventional concrete (Control) were made in accordance with ASTM C-31 (AASHTO T-23) "Making and Curing Test Specimens". SCC specimens (SCC1, SCC2) were not consolidated externally. The quantity and type of specimens are shown in Table 3.1.

Samples from the three different mixtures were cured along with the girders for approximately 18 hours. The specimens were placed on the side of the girder forms (Figure 3.1). Specimens were then transported and storage outside the laboratory under ambient conditions until testing.

3.5 Test Methodologies

3.5.1 On-site Instrumentation

3.5.1.1 Temperature Measurement

Temperature gradients were monitored within the girders during the first 14 hours after casting using Type K thermocouples (Omega FF-K-24). One thermocouple was placed in the top flange, one in the middle (web) and one in the bottom flange for each girder in the test program. In addition, two more thermocouples were used during the curing period to record the ambient temperature and the temperature under the tarpaulin cover. Figure 3.2 shows the locations of the instrumented cross-sections. The thermocouples were

(a) (b)

Figure 3.1 Placing of specimens on the side of the girder forms for curing. The specimens are placed on the side of the girder forms to keep the curing temperatures for the specimens as close as possible to those of the actual girder

connected to a multi-channel recorder (Fig 3.4) that continuously recorded the thermocouples readings until approximately 850 minutes after the first girder was cast.

3.5.1.2 Prestress Measurement

Four Strainsert model PC-50 (50,000 lb capacity) load cells were placed on four strands on the dead end of the casting bed (Figure 3.5). The load cells permitted measurement of the prestressing force after the jack was removed, after curing, and immediately prior to detensioning the strands. Figure 3.2 shows the location of the load cells for the girders.

3.5.2 Fresh Concrete Properties

Sampling of freshly mixed concrete was performed for the three different mixtures in accordance to ASTM C-172 (AASHTO T-141) prior to the casting of the girders. Tests on fresh conventional concrete included unit weight, slump and air content in accordance with ASTM C-138 (AASHTO T-121), ASTM C-143 (AASHTO T- 119) and ASTM C-173 (AASHTO T-152) respectively. Tests on fresh SCC included unit weight in accordance with ASTM C-138 (AASHTO T-121), air content with pressure air meter in accordance with ASTM C-173 (AASHTO T-152), and slump flow test in general accordance with a proposed ASTM test. Fresh SCC was also tested using J-ring and L-box.

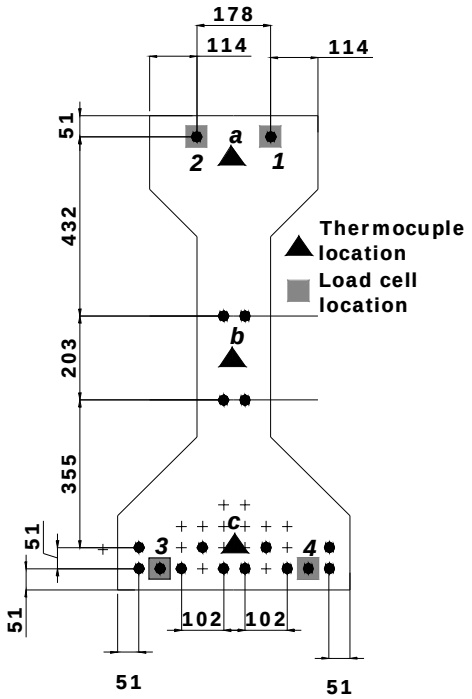

Figure 3.2 Location of thermocouples and load cells. Location of thermocouples at top flange (a), middle (b) and bottom flange (c) of the girder. Location of load cells placed on four selected strands (1,2,3 and 4)

(a) (b)

Figure 3.3 Thermocouple installation. a) attachment to distribute the three thermocouples to the respective location. b) thermocouple attached to the rebar at bottom flange

(a)

(b)

Figure 3.4 Thermocouples connection. a) Connection of thermocouples to multi-channel recorder b) Multi-channel recorder for continuous reading.

(a)

(b)

(c)

Figure 3.5 Load cells installation on four strands on the dead end of the casting bed. a) General set up of load cells and reading box. b) Load cells at top strands. c) Load cells at bottom strands

3.5.3 Mechanical Properties

3.5.3.1 Compressive strength

Compressive strength was determined using cylinders specimens of 4x8 inches at 7 and 28 days for the three different concrete mixtures. The cylinders were tested in accordance with ASTM C39-83 b (AASHTO T 22-86). In order to have plane ends, the cylinders were ground on both top and bottom ends. The cylinders were tested on a 400 kip capacity compression machine as shown on Figure 3.6.

3.5.3.2 Modulus of Elasticity

Elastic modulus was determined using the same cylinder specimens later tested to failure in compression. Two Linear Variable Differential Transformers (LVDT) indicated the axial deformation during loading. The LVDTs measured the displacement of the bottom platen and were placed diametrically opposite to each other (Fig. 3.6). A data acquisition system recorded the output of both gages continuously. These values were averaged and divided by the length of the cylinder to obtain the strain. The load and the strain of the elastic portion of the curve (less than 0.4 f'_c) were used to compute the elastic modulus. Figure 3.6 shows a specimen with the LVDTs prior to testing. As discussed in Chapter 4, this method of measuring the strain was not reliable.

The modulus of elasticity was also obtained based on the measured camber of the three test girders at the time of prestress release as explained in Chapter 2. The average of the readings from the load cells installed on the strands was used as the initial prestress force.

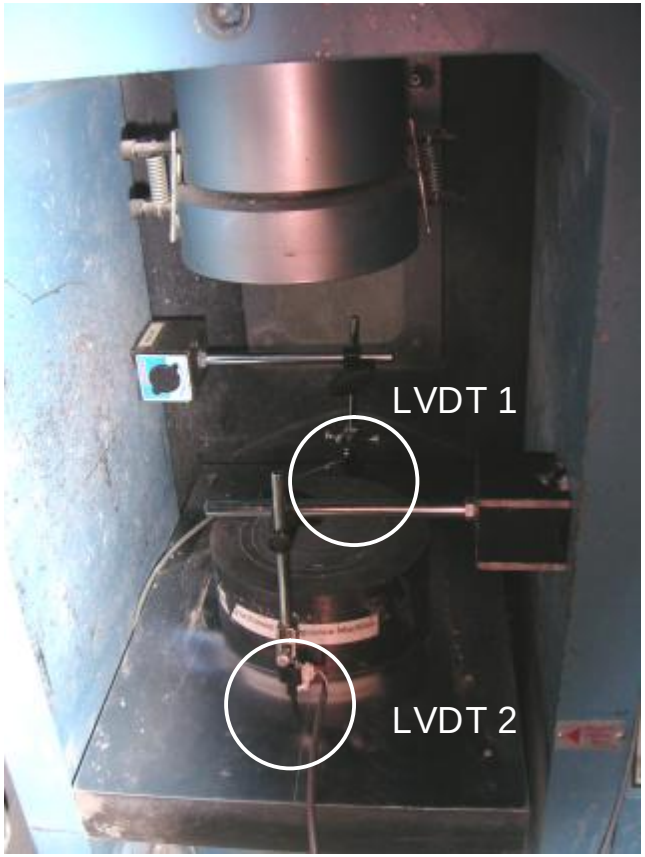

(a)

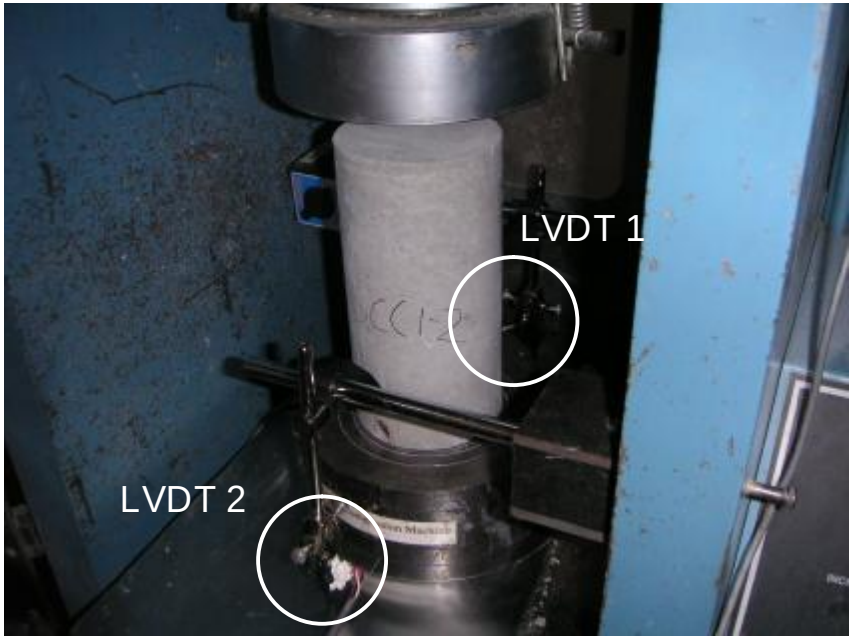

(b)

Figure 3.6 Compressive strength and modulus of elasticity test. a) LVDTs between the top and bottom plates, placed diametrically opposite each other to measure the displacement. b) Same configuration as in a) with a concrete specimen

The elastic modulus for the three mixtures were obtained from creep specimens at the time of loading at 90 days. The strains were measured while loading the test frame. The elastic modulus for each mixture was also obtained from the actual test of the three girders (Section 3.6).

3.5.3.3. Creep

The specific creep of the concrete was determined by measuring strain over time of concrete cylinders loaded in a creep frame in accordance with ASTM C512-87. One frame was used for each mixture (Fig. 3.7). Creep was also obtained using the initial camber measured at the moment of release and the camber at 98 days.

A constant load equivalent to 40% of the strength at 7 days for each of the three different concrete mixtures was applied to each set of creep specimens. The corresponding stress applied to each set of creep specimens was 1,870 psi (12.9 Mpa), 2,310 psi (15.9 MPa), and 2,630 psi (18.1 MPa) for Control, SCC1 and SCC2 respectively. Three 4 x 8 inches cylinder specimens and two 6 by 12 inches high strength concrete cylinders were placed in the frame as shown on Figure 3.7. The cylinders had been previously ground to obtain two smooth, parallel loading surfaces. Two unloaded companion cylinders for each mixture were stored beside the creep frame to permit correcting the total strain by shrinkage strain to determine creep strain. The load was uniformally applied by a hydraulic ram and then transferred to the cylinders by tightening three nuts. A previously calibrated load cell was used to determine the applied load during loading.

(a) (b)

(c)

Figure 3.7 Loaded frames for creep measurement. a) Loaded frames for creep measurements for Control C, SCC1 and SCC2 b) Loaded frame for one admixture showing the plate and bolts c) Loaded frame showing the brass inserts and Demec point.

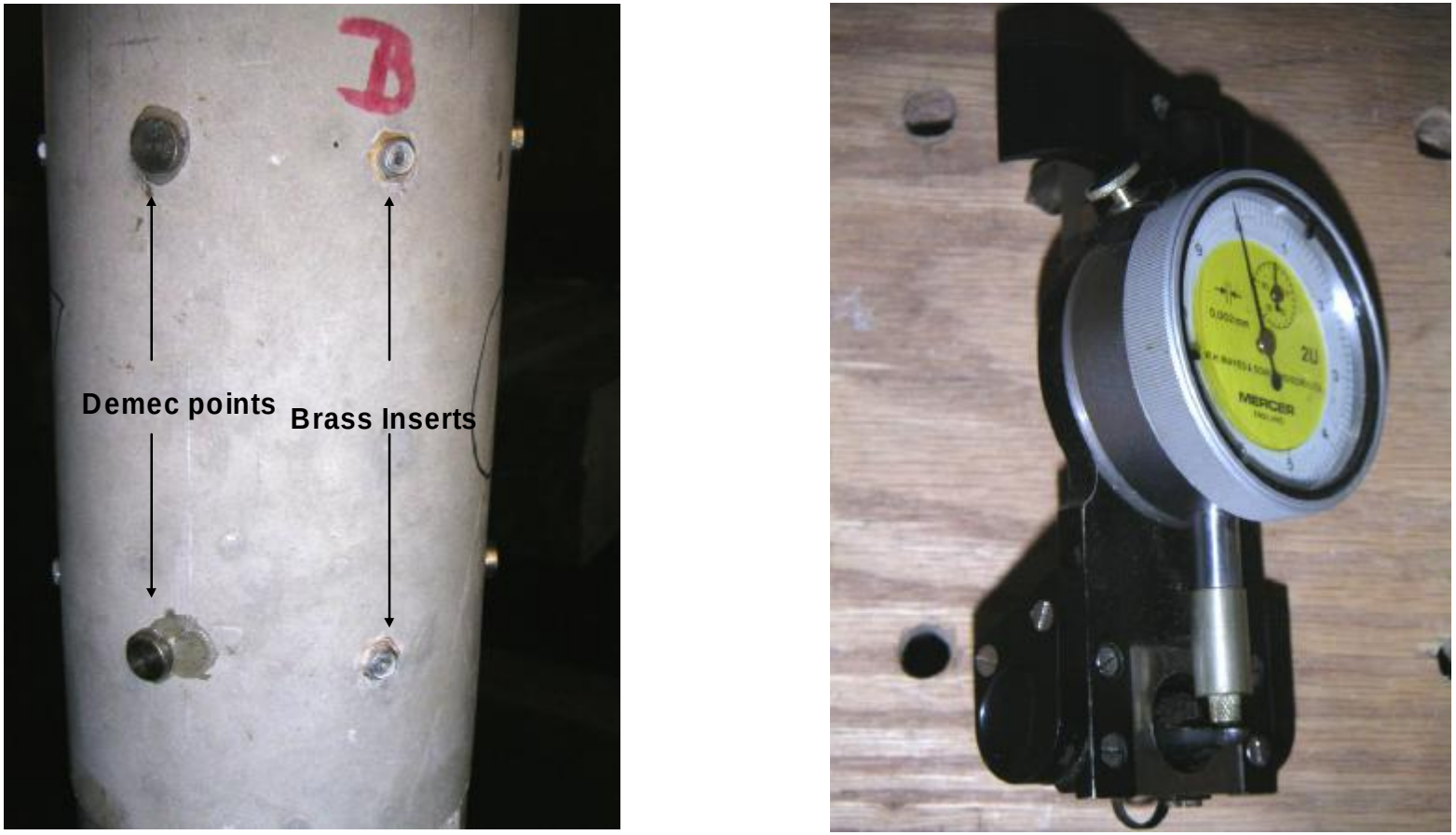

(a) (b)

Figure 3.8 Detail of brass inserts, Demec points and mechanical gage. a) Detail of brass inserts and Demec points for creep measurements b) Mechanical gage indicator used for creep measurements.

Six brass inserts were installed within the samples as shown on Figure 3.8. The three pairs of inserts were placed within a separation of 120° between them. A mechanical Demec strain indicator (Fig. 3.8) was used to determine the length between the pairs of inserts in both the loaded and unloaded companion cylinders.

Demec measurements were taken daily for the first week after loading and once a week thereafter. Discrepancies within the acquire creep data led to review the test method and equipment, including the brass inserts cast into the cylinders. Each frame was unloaded at 60 days after initial loading, and six new Demec points were attached to each cylinder using epoxy, to provide more accurate readings. The creep frames were reloaded to the original load at 90 days. Measurements using the new Demec points were performed every other day for the first week and once a week therefore.

3.5.3.4 Shrinkage

Shrinkage measurements on 4x8 in cylinders used as companion cylinders during the creep test had the discrepancies explained in section 3.5.3.3. Measurements using the new Demec points were performed every other day for the first week and once a week therefore. The specimens were stored at laboratory conditions.

Four shrinkage prisms were fabricated for two mixtures while casting the girders. Only the control and SCC2 mixtures were tested for shrinkage due to an insufficient amount of SCC1 mixture. Since these samples were stored outside the laboratory in ambient conditions, without temperature control, the change in volume including thermal

(a)

(b)

Figure 3.9 Shrinkage Measurement configuration. a) Shrinkage stand with electronic gage based indicator and calibration bar. b) Shrinkage prisms sample on shrinkage stand

expansion/shrinkage and drying shrinkage were measured together. The volume change was measured in accordance with ASTM C 490-89 using an electronic gage based indicator reading to the nearest 0.0001 inches (Figure 3.9). Length measurements were taken daily for the first week, once a week for a month and once a month thereafter.

3.5.3.5 Dynamic Modulus of Elasticity.

The dynamic modulus test of concrete disks was conducted as described in Leming, ***et al***, [1998], using the fundamental cyclic natural frequency of the disks. The fundamental cyclic natural frequency of the disk was determined experimentally using a small, piezoelectronic accelerometer connected to one side of the specimen with a soft, adhesive wax with good acoustical properties. The disk was exited by striking it with a steel ball. To allow free free-vibration, the disk was air suspended vertically using a sling.

The signal from the accelerometer was captured at a sampling rate of 100 kilohertz. The signal was analyzed after removing the portion of the signal immediately following the impact of the ball-bearing. The fundamental frequency was identified using Fast Fourier Transform (FFM) techniques. A minimum of three tests was conducted on each disk. The thickness and diameter of each disk was determined with micrometers. Measurements were taken at several points. The bulk mass density of the concrete specimens was determined from air-dry and immersed mass measurements, following the procedures outlined in ASTM C 29 [ASTM, 2002].

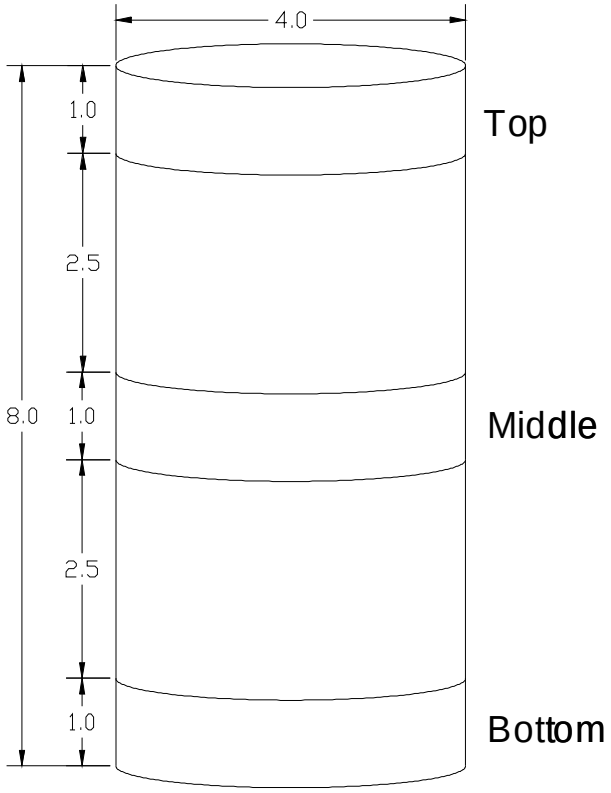

Figure 3.10 Schematics of a 4 x 8 in specimen used for dynamic modulus of elasticity and air permeability index

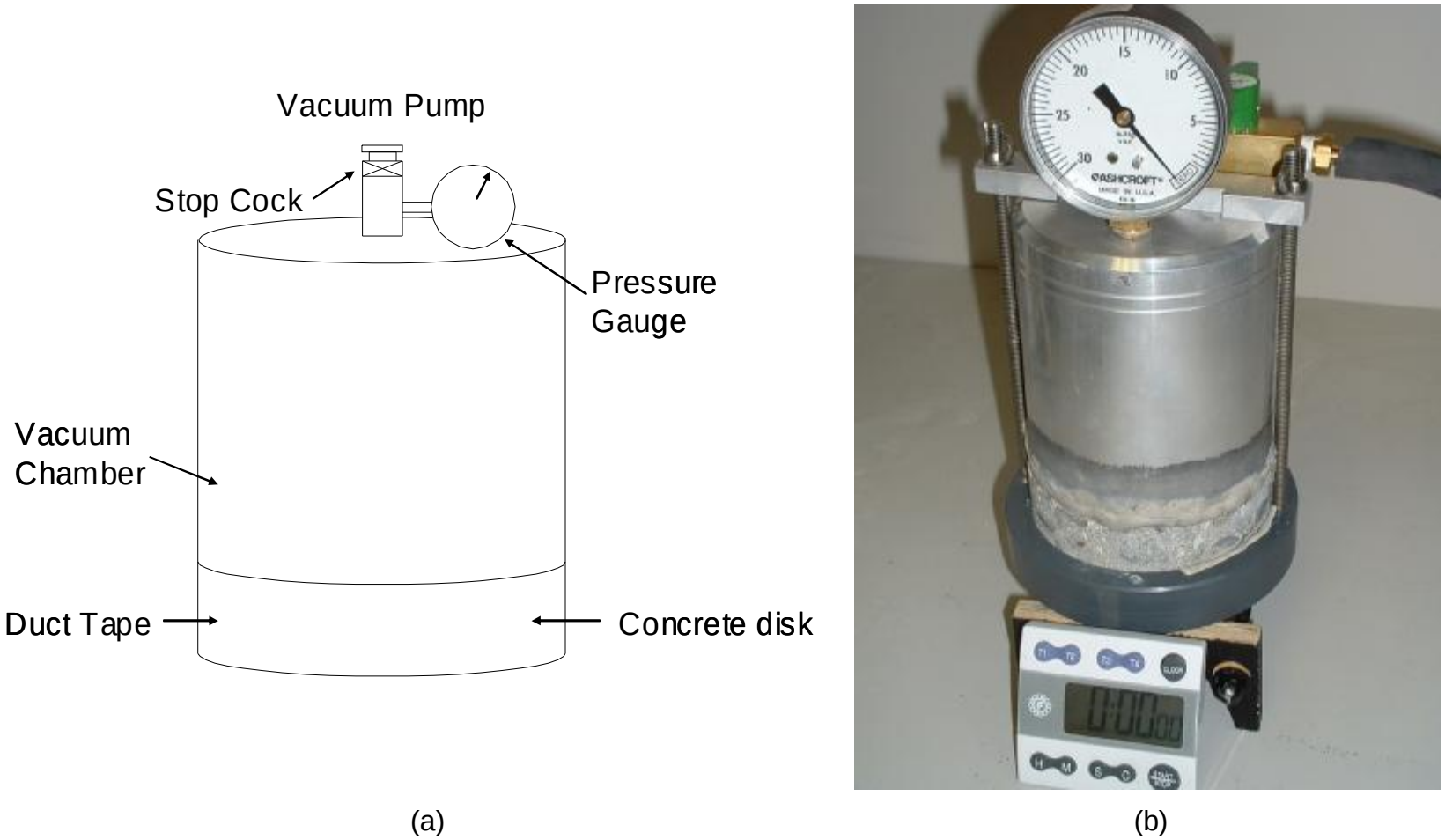

Figure 3.11 Air permeability index apparatus a) Schematics of Air Permeability Test Apparatus. b) Air Permeability Test Apparatus

Concrete disks were originally made in the field at the same time as cylinder specimens. Plastic cylinders molds, 4 inches in diameter had been previously cut transversally to obtain 4 in by 1 in. Disk molds. Disks samples were also obtained by sawing 4 by 8 concrete cylinders top, middle, and bottom of the sample (Figure 3.10) for examination of potential segregation.

3.5.3.6 Permeability Testing

The air permeability index was determined based on the method reported by Scholin and Hilsdorf [1998]. A vacuum chamber was placed on the top surface of a 1 in (25 mm) thin disk. The side of the disks was taped so that air could enter only through the lower face of the disks. The chamber was evacuated with a vacuum pump which firmly seated the specimen. After the stopcock is closed between the vacuum chamber and the pump, the air pressure increases inside the chamber as air penetrates through the sample. Once a stable vacuum was obtained, the valve of the vacuum pump was closed and the time required for the pressure to fall from about 29.0 in Hg (980 milibars) to 27.0 in Hg (914 milibars) was determined. The test was conducted twice for each specimen. The time for the given change in pressure was determined using a stopwatch.

The vacuum chamber used in this study is shown in Figure 3.11. The test chamber was constructed of metal and had a volume of 460 ml. The chamber was sealed to the sawed face of the concrete disk using a thin strip of soft clay. This method had been used successfully in previous studies [Leming and Guth, 1998, Leming and Savas 2000].

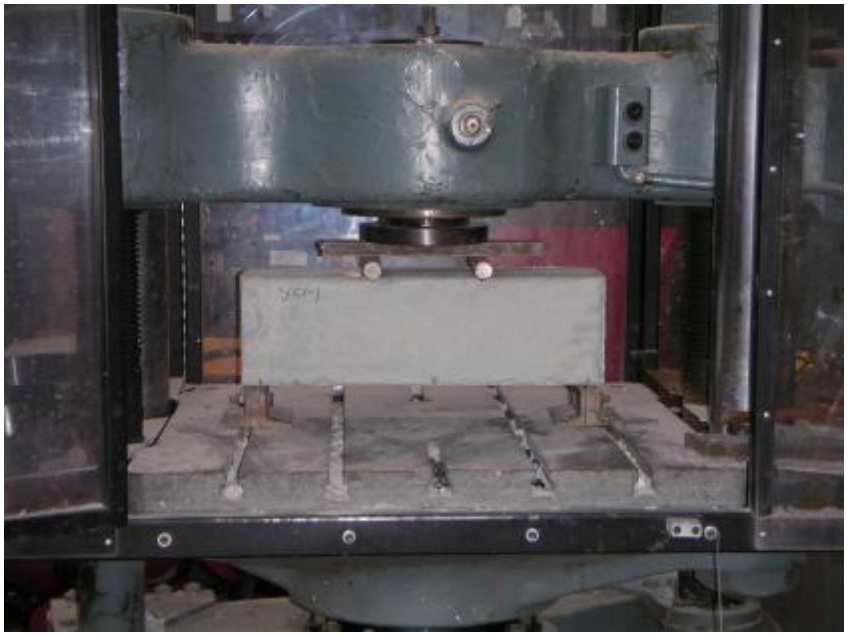

(a)

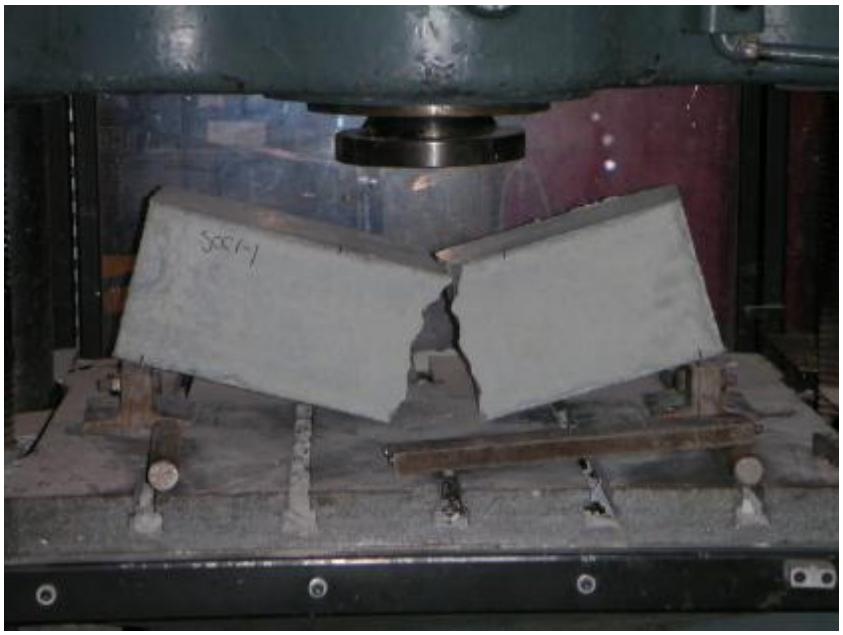

(b)

Figure 3.12 Modulus of rupture test. a) Modulus of rupture specimen before loading. b) Fractured modulus of rupture specimen

3.5.3.7. Modulus of Rupture

The modulus of rupture was determined using six 152 x 152 x 508 mm (6 x 6 x 20 in) prisms tested at 28 days (Fig 3.13). Two prisms from each mixture were tested in accordance with ASTM C 78-84 (AASHTO T 97-86).

3.6 Test of Girders at Full Service Load Conditions

Static load tests of the two SCC girders and the non-SCC girder were performed up to full service load conditions at S&G Prestress, Wilmington, North Carolina, 90 days after casting. A test load frame was supplied by S&G Prestress (Fig 3.14)

The load was applied by a hydraulic jack at top mid-span and displacement was recorded by two dial gages close to the side of the girder (Fig. 3.15). Two 1-inch metal plates were placed between the girder and concrete blocks that served as supports on both ends to prevent deflection. Each girder was loaded to 55.8 kips in 6.2 kips increments. Deflection was recorded for the three girders. The elastic modulus was calculated using deflection, moment of inertia, and load data.

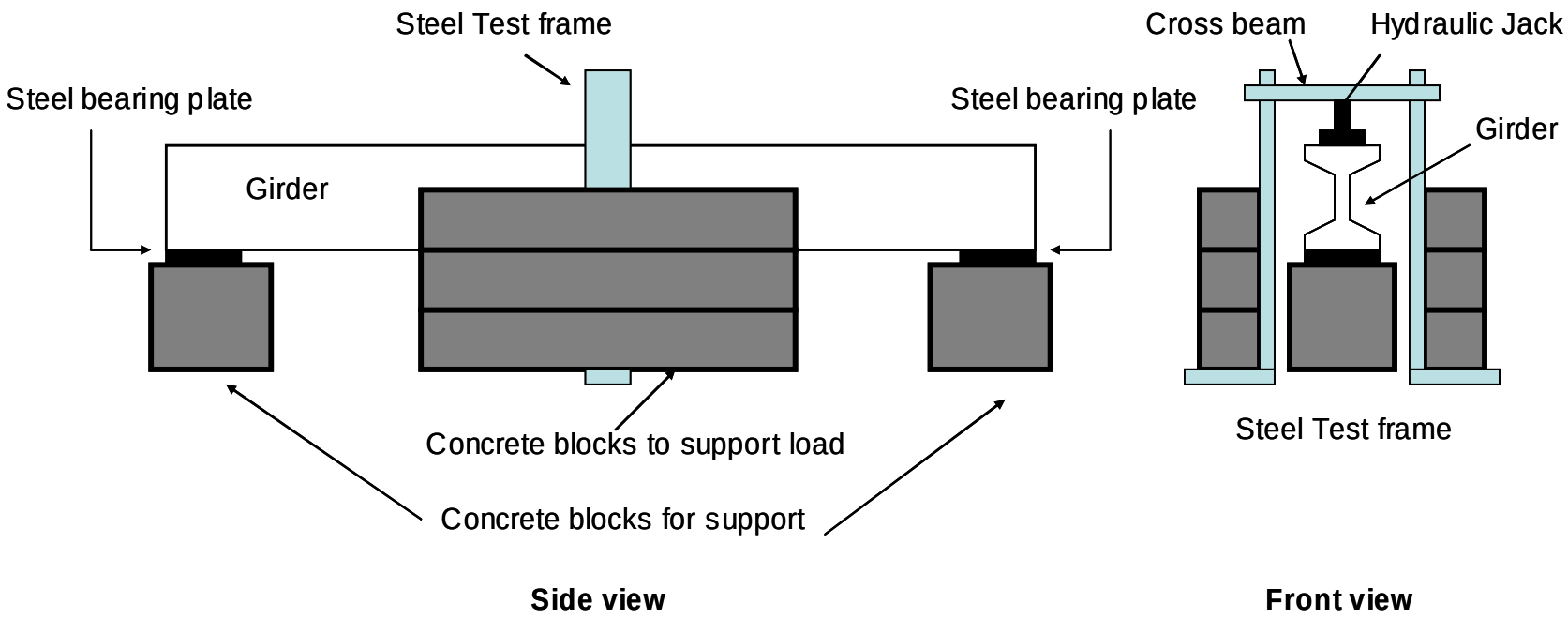

Figure 3.13 Schematics of test frame used to load test the girders at the prestressing plant at Wilmington, NC.

(a)

(b)

Figure 3.14 Test frame used to load test the girders at the prestressing plant at Wilmington, NC. a) 60 tons Hydraulic jack located at mid-span of the girder. b) Front view of test frame

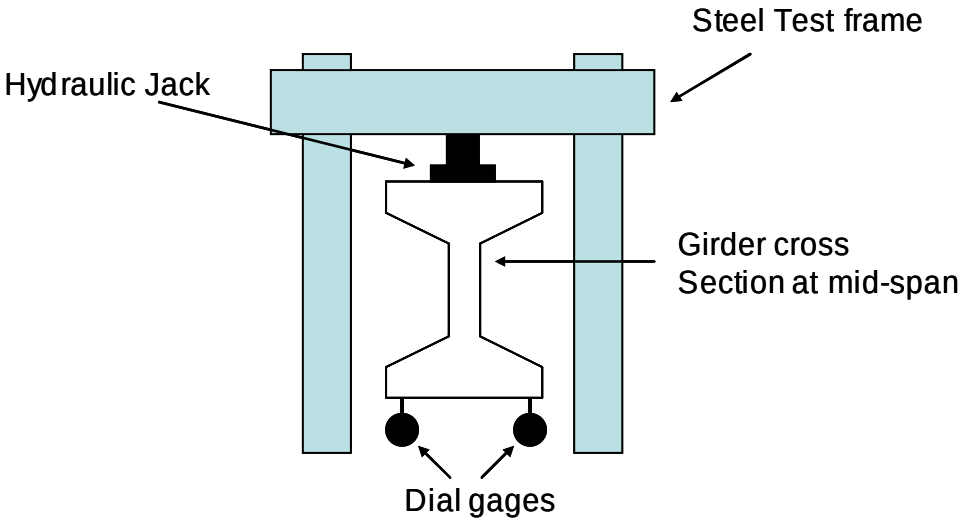

(a)

(b)

Figure 3.15 Schematic of testing at girder mid-span and installation of gages. a) Schematic of girder at mid-span with dial gages. b) Installation of dial gages at mid-span of the girder

CHAPTER 4: RESULTS AND DISCUSSIONS

4.1 Properties of Fresh Concrete

Table 4.1 summarizes the fresh properties of both the conventional concrete and SCC that were measured at the prestress plant. As expected, conventional concrete had a higher unit weight than SCC due to higher coarse aggregate content. Temperature, air content of the three mixtures and slump for the conventional concrete were within the NCDOT specified criteria.

Slump flow for SCC1 and SCC2 were lower than the target values of 26 and 28 in (660 to 710 mm). SCC for both girders was able to flow around the reinforcement and fill all the spaces within the formwork as expected, however. No difficulties were observed during casting of either girder.

Although the mixture proportions for SCC1 and SCC2 were the same, SCC1 had a much higher flow rate than SCC2. The time for SCC2 to reach the 20 in diameter was 3.5 times greater than SCC1. Passing ability using the J-Ring test was also low for SCC2 (VSI=2) and high for SCC1, with a difference of 3 in (76 mm).

These findings indicates that a slump flow value between 23¾ and 24 inches, although lower than the target values, provided adequate flowability to deform and spread freely for filling all the spaces of the formwork. Khayat, *et al.* [2004], report that slump flow values around 24 are considered acceptable.

Table 4.1 Properties of Fresh Concrete

Properties	**C**	**SCC1**	**SCC2**
Unit weight, lbs/ft^3	147	142	142
Concrete Temperature, F	88.2	91.8	89.6
Air Content, %	3.4	4	5.7
Slump, in	6	N/A	N/A
Slump Flow, in	N/A	24	23¾
Visual Stability Index (VSI)	N/A	1 (stable)	1 (stable)
Flow Rate & Viscosity, t50 in s	N/A	1.6	5.6
J-Ring Flow, in	N/A	23.5	20.5
Passing Ability Index	N/A	0 (high)	2 (Low)
Blocking Ratio, H2/H1	N/A	0.5	0.52

Table 4.2 Properties of Hardened Concrete

Age	**Control C**	**SCC1**	**SCC2**
Compressive strength f'_c (psi)			
18 hrs	4,700	5,550	5,450
7 days	6,600	8,980	7,440
28 days	7,280	10,970	10,540
Flexural Modulus			
28 days	570	550	550
Static Modulus of Elasticity (Mpsi)			
7 days	2.40	1.70	1.60
28 days*	3.00	3.50	3.20
90 days**	4.30	4.40	4.70
98 days***	4.60	4.70	4.40
Dynamic Modulus of Elasticity (Mpsi)			
28 days	4.77	5.34	5.07

* Not standard cure

** Based on elastic measured at loading for creep test

***Based on load test of girders

No segregation of the mixture was observed during the slump flow test. Visual inspection of the circular spread determined that SCC1 and SCC2 had a Visual Stability Index (VSI) value of one. While positive, the visual observation on the slump flow test did not offer conclusive information regarding segregation.

The difference between the flow test and the J-ring for SCC1 and SCC2 was 0.5 inches and 3.3 inches respectively. As noted in Chapter 2, both mixtures exceeded the difference suggested by EFNARC of 0.4 inches. The difference for SCC2 between the flow test and the J-ring was even greater than the 2 inches that were previously proposed by EFNARC for a mixture to pass through the reinforcement successfully. Regardless of these values, both SCC2 and SCC1 were apparently able to flow around the reinforcement and fill the spaces within the formwork.

As shown in Table 4.1 the blocking ratio (h2/h1) based on the L-box test was very similar for both SCC1 and SCC2. For both mixtures, the blocking ratio was lower than the 0.8 limit proposed by the EFNARC guidelines for SCC. Although a high variability was found between the two SCC mixtures, no apparent difference in performance was found. These results suggest that more research is needed for testing fresh properties of SCC and for specifications to successfully achieve SCC.

4.2 Concrete Curing Temperature

Figures 4.1, 4.2 and 4.3 show the curing development of the three test girders, the temperature under the tarpaulin cover, and the ambient temperature. The temperature in

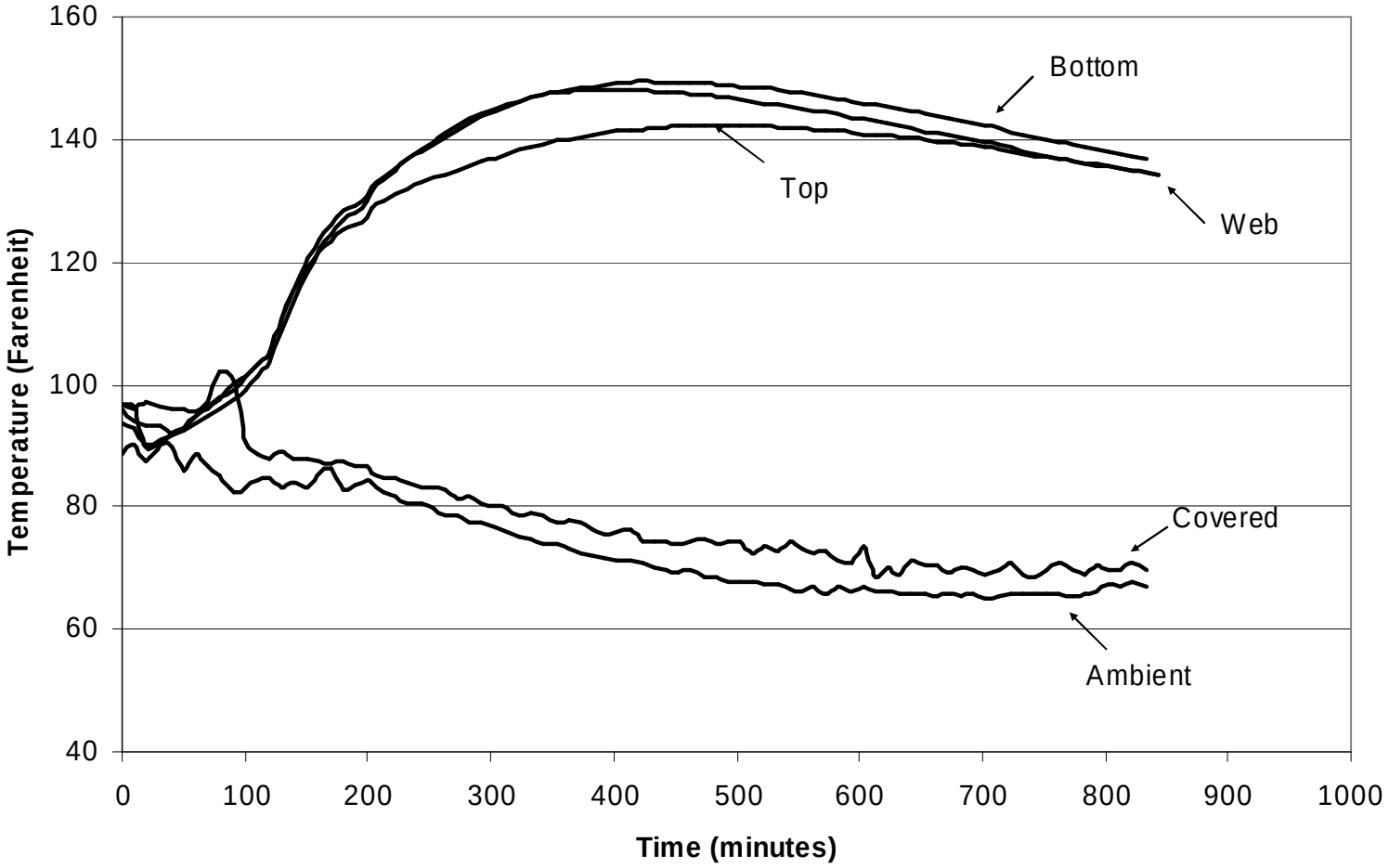

Figure 4.1 Concrete curing temperatures for Control C girder

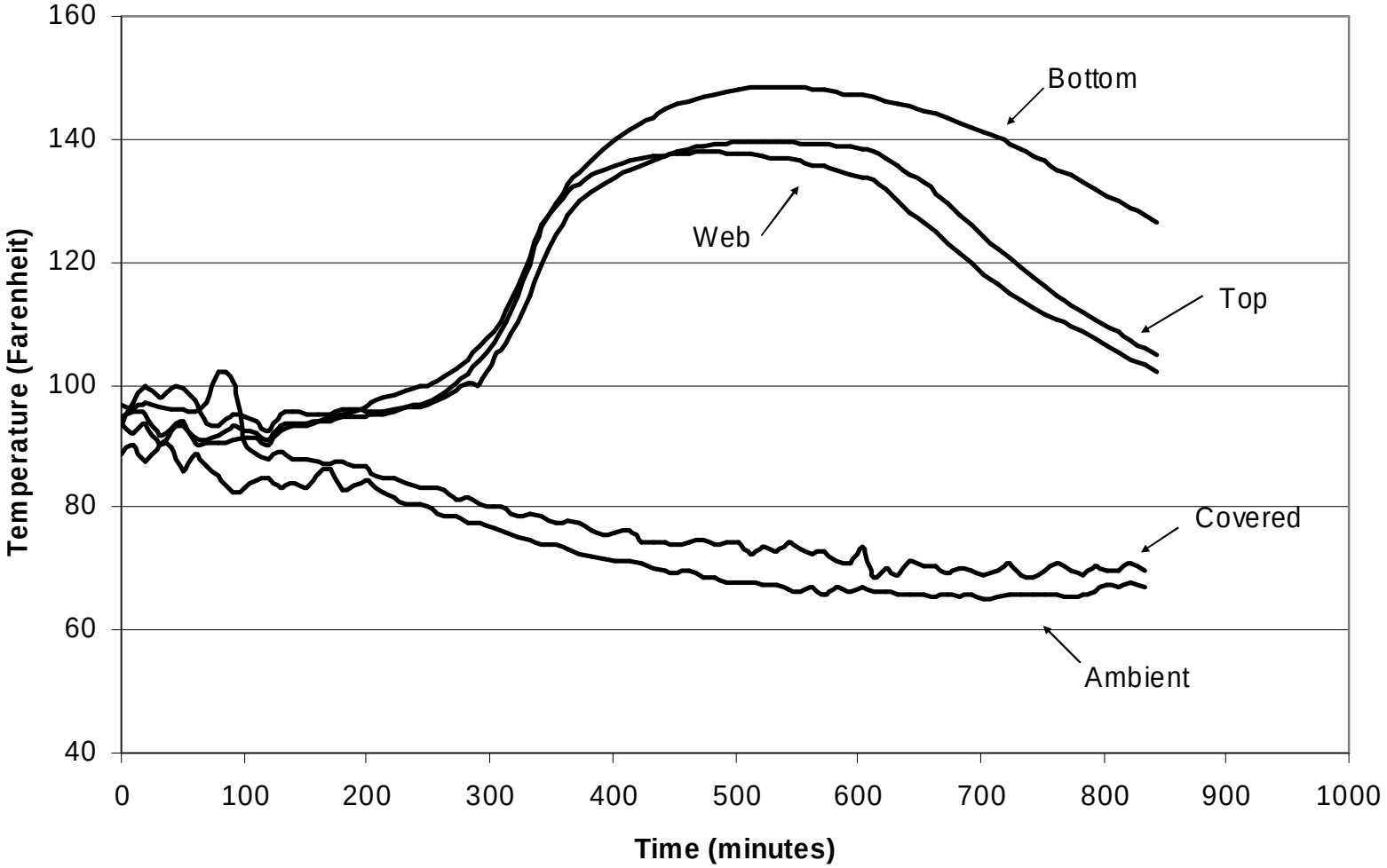

Figure 4.2 Concrete curing temperatures for SCC1 girder

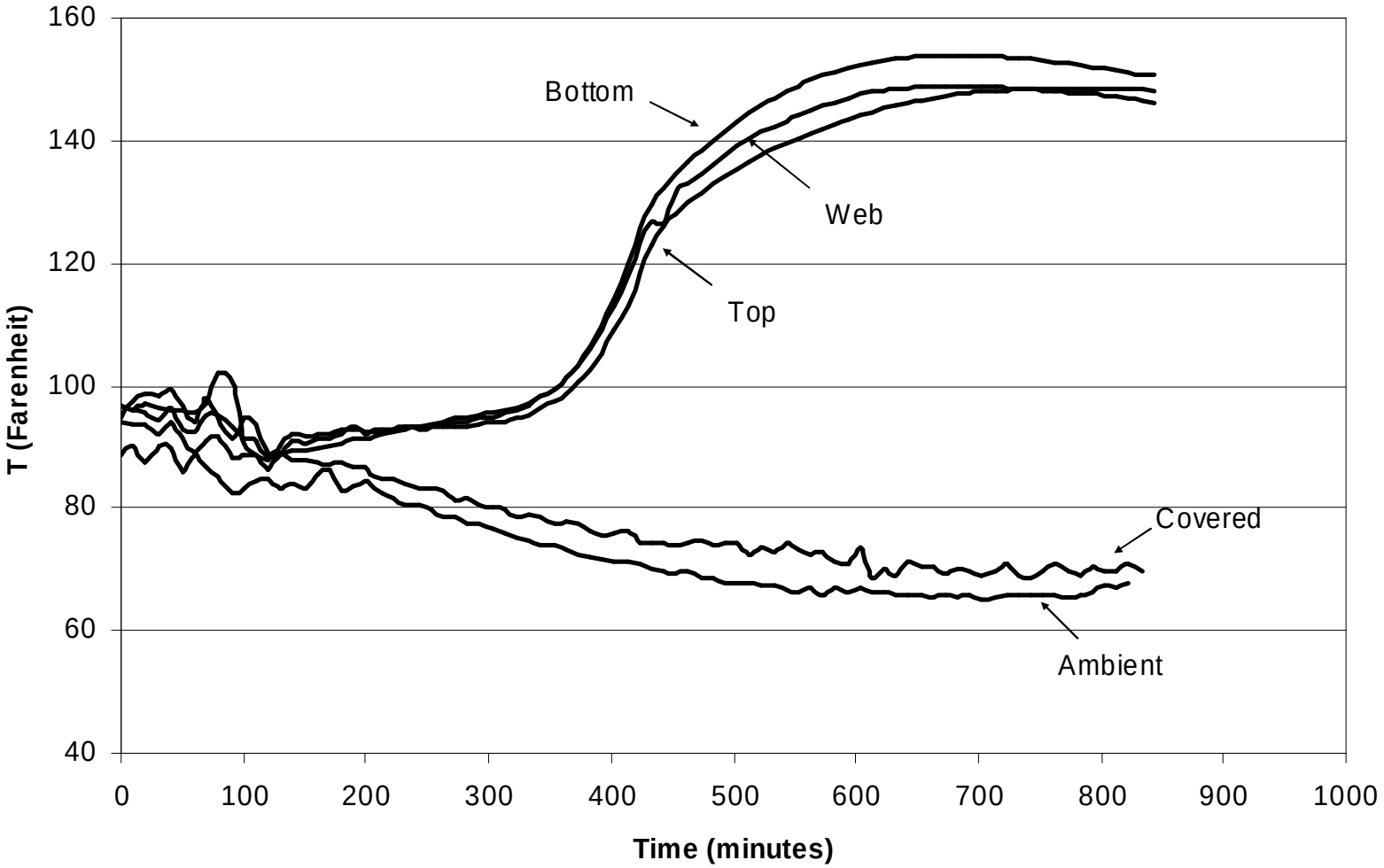

Figure 4.3 Concrete curing temperatures for SCC2 girder

the bottom flange was slightly higher than that in the web and in the top flange, but the difference was small. The temperature under the tarpaulin cover and the ambient temperature were quite similar, and they dropped to as low as 70°F at night.

Figures 4.1, 4.2 and 4.3 show that the curing temperature for the Control C girder and both SCC girders were practically the same, except for the time required to reach the peak temperature, which represent the difference in time between the consecutive castings of the three girders. Temperature records indicate that regardless the higher cement content of the SCC mixtures, practically no difference in temperature was found between conventional concrete and SCC.

4.3 Initial Prestressing Force

Four load cell readings from the selected strands are summarized in Table 4.3. Based on the average of the load cell readings, the initial tension may be taken as 30,090 lbs per strand. Just before detensioning, the average of the load cell readings was 29,640 lbs due to strand relaxation. The initial prestressing force applied to the girders was therefore taken as 29,640 lbs per strand.

4.4 Properties of Hardened Concrete

Results for compressive strength, flexural modulus, static modulus of elasticity and dynamic modulus of elasticity are shown in Table 4.2. Each result represents the average of two specimens except for the dynamic modulus, which represent the average of three disk specimens.

Table 4.3 Load Cell Readings

Load Cell	Load Cell Reading (lbs)			
	Initial tension	**19 hrs after initial**	**43 hrs after intial**	**48 hrs after initial (Just before detensioning)**
# 1	29,600	29,700	28,800	28,900
# 2	29,800	29,600	28,800	28,800
# 3	30,200	30,100	29,700	30,100
# 4	30,770	30,770	30,570	30,770
Average	**30,090**	**30,040**	**29,470**	**29,640**

Table 4.4 Camber Growth and Creep Coefficient of Test Girders

Test Girder	Initial camber	Camber @ 98 days	Camber Growth	Creep Coefficient
Control	0.25"	0.94"	0.69"	2.76
SCC1	0.25"	1.25"	1.00"	4.00
SCC2	0.25"	2.00"	1.75"	7.00

Note: Creep coefficient = Growth of camber/Initial Camber

Table 4.5 Comparison of Specific Creep

Test Specimen	Control C	SCC1	SCC2
Specific Creep from Loading at 90 Days (A)	0.072 x 10-6 per psi	0.068 x 10-6 per psi	0.081 x 10-6 per psi
Specific Creep from Initial Loading (B)	0.628 x 10 - 6 per psi	0.910 x 10-6 per psi	1.593 x 10-6 per psi
Ratio A/B	0.114	0.075	0.051

4.4.1 Compressive Strength and Flexural Modulus

Development of concrete strength was consistent for both the conventional concrete and SCC. An early compressive strength in excess of 4,000 psi (27.6 MPa), needed for prestress release, was reached within 18 hours and both concretes reached the specified 28-day strength of 5,000 psi (34.5 MPa), exceeding 7,000 psi (48.3) and 10,000 psi (69.0 MPa), for conventional concrete and SCC, respectively. As expected, SCC compressive strength at 28-days was greater due to the higher cement content. Flexural strength was similar for both concretes. Values are shown in Table 4.2.

4.4.2 Modulus of Elasticity

The static Modulus of Elasticity (E_c), determined using 4x8 in (102 x 204 mm) cylinders at different ages, was lower than expected for both conventional concrete and SCC. Values of 2.4 Mpsi and 1.65 Mpsi were recorded at 7 days for conventional concrete and SCC respectively. At 28 days, SCC had a higher E_c than the conventional concrete, as expected due to higher strength, but still much lower values than expected for concrete with similar compressive strength (Table 4.2).

It is believed that two main factors may have affected the results for E_c. The coarse aggregate that was used in both mixtures was a low porosity granite which would have contributed to a higher E_c. However, the manufactured marine marl limestone with high porosity and low stiffness was used as fine aggregate for both mixtures. Due to the higher

content of fine aggregate for SCC, it is expected that SCC would have a lower E_c than the control concrete, which is the case for 7 days.

At 28 days much of the hydration process of concrete has been completed. The microstructure of the paste matrix and the transition zone at this age has improved and porosity has been reduced. Since all the specimens were fabricated in the casting plant under the sun and were not moist cured, the paste matrix and the transition zone were more porous than under standard conditions. Additional work in this study using conventional concrete cylinders showed that the E_c at 21 days of moist cured specimens were approximately 0.5 Mpsi higher than specimens from same concrete batch that were air cured.

Although these two factors may have affected to some degree the elastic moduli of the conventional concrete and SCC, the values obtained from testing the cylinders, at 7 and 28 days, are much lower than normally expected for concrete of similar compressive strength.

The elastic moduli for the conventional concrete and SCC can also be obtained by using the camber of the three girders at the time of prestress release. The strand force just before detensioning can be obtained from the force measured by the four load cells

$$f_{average} = \frac{28{,}900 + 28{,}800 + 30{,}100 + 30{,}770}{4} = 29{,}640 \text{ lbs/strand}$$

The initial prestressing force for 18 strands is

$$P_i = 18(29{,}643) = 533{,}574 \text{ lbs}$$

$$e = 8.83\,\text{in} \qquad I = 125{,}390\,\text{in}^4$$

From Equation 2.10, the camber due to $P_i e$ can be obtained as

$$\Delta_1 = \frac{P_i e l^2}{8EI} = \frac{(533{,}574)(8.83)(54.79\times 12)^2}{8E(125{,}390)} = \frac{2{,}030{,}334}{E} \uparrow \text{lbs/in}$$

From Equation 2.17, the deflection due to dead load is

$$\Delta_2 = \frac{5wl^4}{384EI} = \frac{5(583)(54.79)^4(1728)}{384E(125{,}390)} = \frac{942{,}143}{E} \downarrow \text{lbs/in}$$

the net camber is obtained from Δ_1-Δ_2:

$$\Delta_{net} = \frac{2{,}030{,}334 - 942{,}743}{E} = \frac{1{,}087{,}591}{E} \text{ lbs/in}$$

The initial camber was measured as soon as the strands were released. The initial camber of 0.25 in was the same for the three test girders:

$$E = \frac{1{,}087{,}591}{0.25} = 4.35\times 10^6 \text{ psi}$$

If a 4% loss of prestress due to elastic shortening is assumed and the span is 54.79 from end to end then

$$\Delta_1 = \frac{(533{,}574)(8.83)(54.79\times 12)^2(0.96)}{8E(125{,}390)} = \frac{1{,}949{,}121}{E} \uparrow \text{lbs/in}$$

$$\Delta_2 = \frac{5(583)(54.79)^4(1728)}{384E(125{,}390)} = \frac{942{,}143}{E} \downarrow \text{lbs/in}$$

$$E = \frac{1{,}949{,}121 - 942{,}743}{0.25} = \frac{1{,}006{,}378}{0.25} = 4.03\times 10^6 \text{ psi}$$

The elastic moduli for the conventional concrete and SCC were also obtained by using the initial elastic strains that were measured from the loaded creep specimens at 90 days.

Table 4.6 Stress-Strain Values from Creep Specimens

	Stress (psi)	**Microstrain**
Control	1,870	437
SCC1	2,310	525
SCC2	2,630	555

Table 4.7 Dynamic Modulus of Elasticity at Different Depth

Dynamic Modulus of Elasticity (Mpsi)			
Location	**Control**	**SCC1**	**SCC2**
Top (1 in)	4.64	5.57	5.18
Middle (4 in)	5.01	5.49	5.32
Bottom (8 in)	5.06	5.52	5.23
% T-B	8.94	-0.90	0.97

Table 4.8 Air Permeability Index of Disk Specimens and Air Permeability Index at Different Depths

Mixture	**API-Cast (m^2/s)**	**API-Sawn (m^2/s)**		
		Top (1 in)	**Middle (4 in)**	**Bottom (8 in)**
Control	0.080	0.041	0.032	0.047
SCC1	0.047	0.023	0.005	0.028
SCC2	0.035	0.030	0.004	0.011

Table 4.6 shows the strain and the corresponding stress applied to each set of creep specimens. From equation 2.1:

$$E = \frac{1870}{437\times10^{-6}} = 4.3\times10^{6}\ \text{psi}$$

$$E = \frac{2310}{525\times10^{-6}} = 4.4\times10^{6}\ \text{psi}$$

$$E = \frac{2630}{555\times10^{-6}} = 4.7\times10^{6}$$

for Control C, SCC1 and SCC2 respectively.

As shown in Table 4.2, the elastic modulus for the conventional concrete and SCC mixtures was also obtained at 98 days by testing the three girders at approximately 40% of service load (Section 4.6). The results differ from those obtained with the cylinders specimens loaded at 28 days and, as expected, are more consistent with those obtained by measuring the camber of the three test girders at the time of prestress release and those obtained during the loading stage for creep tests.

These results indicate that the elastic modulus obtained from the 4x8 inches cylinder at 7 and 28 days may not be reliable due, most probably, to measuring the displacement of the bottom platen of the compression testing machine. As discussed in Chapter 3.5.3.2, by measuring only platen movement, any strain in the system would be interpreted as strain in the concrete; a higher imputed strain would result in a lower measured elastic modulus.

The difference in strength is largely responsible for differences in the elastic modulus. Table 4.9 shows the estimated elastic modulus using the ACI equations (Chapter 2) and

Table 4.9 Elastic Modulus Estimation Using ACI Equations at 18 hrs and 90 Days. Calculation of Constant *k* from ACI Equations for Control and SCC E_c Comparison (Strength Adjustment)

			Control	SCC1	SCC2
			Ec Estimated using ACI equations (Mpsi)		
		f_c 18 hours	4,700	5,550	5,450
		f_c 90 days*	8,010	12,070	11,590
ACI 318	$E_c = w^{1.5}33\sqrt{f'_c}$	18 hrs	4.0	4.2	4.1
		90 days	5.3	6.1	6.0
ACI 318	$E = 57{,}000\sqrt{f'_c}$	18 hrs	3.9	4.2	4.2
		90 days	5.1	6.3	6.1
ACI 363	$E = 40{,}000\sqrt{f'_c} + 10^6$	18 hrs	3.7	4.0	4.0
		90 days	4.6	5.4	5.3
				E_c (Mpsi)	
Based on initial camber		18 hrs	4.0	4.0	4.0
Based on creep load		90 days	4.3	4.4	4.7
Based on load test		98 days	4.6	4.7	4.4
			Constant values using Ec at 90 days		
ACI 318	$E_c = w^{1.5}k\sqrt{f'_c}$	*k* 90 days**	27	24	26
		k 98 days***	29	25	24
ACI 318	$E = k\sqrt{f'_c}$	*k* 90 days**	48,000	40,100	43,700
		k 98 days***	51,400	42,800	40,900
ACI 363	$E = k\sqrt{f'_c} + 10^6$	*k* 90 days**	36,900	30,900	34,400
		k 98 days***	40,200	33,700	31,600

* f_c at 90 days estimated 10% higher than f_c at 28 days, values on psi

** K 90 days based on creep load

***K 98 days based on load test

Table 4.10 Elastic Modulus Comparison Between Conventional Concrete and SCC After Strength Adjustment

				Average differences	
	Age	***k* Control**	***k* Average SCC**	**C-SCC**	**C-SCC**
ACI 318	90 days**	27	25	8.3%	11.3%
	98 days***	29	25	14.3%	
ACI 318	90 days**	48,000	41,900	12.9%	15.7%
	98 days***	51,400	41,800	18.6%	
ACI 363	90 days**	36,900	32,700	11.4%	15.2%
	98 days***	40,200	32,600	18.9%	

Table 4.11 Difference Between Estimated and Measured Elastic Modulus for Conventional Concrete and SCC

					Differences		Average differences	
		***k* Control**	***k* Average SCC**	***k* from ACI**	**C-Est**	**SCC-Est**	**C-Est**	**SCC-Est**
ACI 318	90 days**	27	25	33	18.3%	25.0%	15.5%	25.1%
	98 days***	29	25	33	12.6%	25.1%		
ACI 318	90 days**	48,000	41,900	57,000	15.7%	26.6%	12.8%	26.6%
	98 days***	51,400	41,800	57,000	9.8%	26.6%		
ACI 363	90 days**	36,900	32,700	40,000	7.8%	18.4%	3.6%	18.4%
	98 days***	40,200	32,600	40,000	-0.6%	18.4%		

the adjustment for strength in order to compare E_c between conventional concrete and SCC. Because there was no strength test at 90 days, an increment of 10% was assumed for the strength test value at 28 days; this value is consistent with predicted equations found in ACI 209.

Table 4.10 shows the elastic modulus differences between conventional concrete and SCC after strength adjustment. E_c for SCC was, as expected, approximately 15% lower than conventional concrete at 90 days. This is consistent with the lower coarse aggregate content in the SCC.

Table 4.11 shows that the best model to predict E_c was ACI 363, with a difference of 3.6% and 18.4% for conventional concrete and SCC respectively. This is reasonable due to the high compressive strengths obtained. A difference of 3% does not appear to be significant compared to the difference between predicted and measured E_c. Predicted E_c for SCC, however, shows at least a difference of 18%, which can be significant.

4.4.3 Dynamic Modulus of Elasticity

The dynamic modulus of elasticity (E_d) for Control, SCC1 and SCC2 at 28 days are shown in Table 4.2. Similar to the static modulus, SCC1 and SCC2 show a higher E_d than Control due to higher strength. As discussed in section 4.2.2, the aging of the concrete under air curing did not apparently enhance the modulus of elasticity even though the compressive strengths were improved. Assuming that E_c was similar at 28 and

90 days, the difference between E_c and E_d was 10% for conventional concrete and an average of 13% for both SCC mixtures, which is relatively small.

4.4.4 Dynamic Modulus of Elasticity at Different Depths

The dynamic modulus of elasticity was determined at different depths of test cylinders. E_d values for every specimen and the average of two disk samples are shown on Figures 4.4, 4.5. For the SCC disks, no meaningful difference in mechanical properties were found between the top 1 inch and bottom 1 inch of these cylinders, that is, there was no evidence of segregation.

The difference in E_d between the top and bottom of the cylinder are also shown in Table 4.7. It is useful to note that both SCC1 and SCC2 had virtually no difference in E_d between these two depths, while Control C had a difference of almost 9%.

This is an important finding indicating that the SCC, which received no additional consolidation in the cylinder, showed no evidence of segregation and that, perhaps surprisingly, the conventional concrete which was rodded during fabrication, might have shown evidence of segregation. Based on these findings, it can be reasonable to conclude that the SCC mixtures in this study did not segregate, although additional research is needed to confirm both this approach and these findings. It is important to note that although no segregation was found, the maximum height of the cylinder was only 8 inches. Additional study on segregation using measures such as the column test for SCC should be conducted.

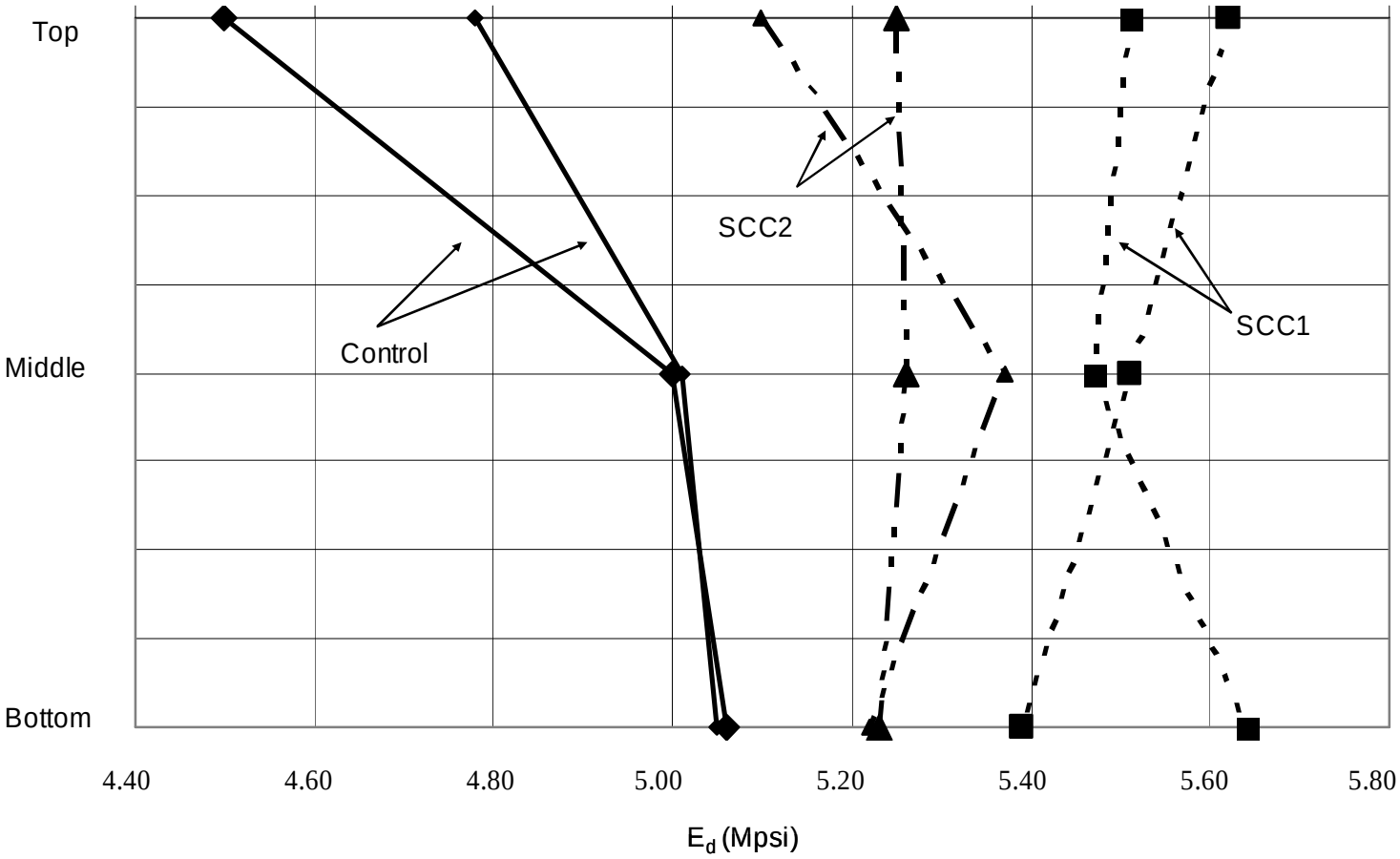

Figure 4.4 Dynamic modulus of elasticity at different depths using two samples for each mixture

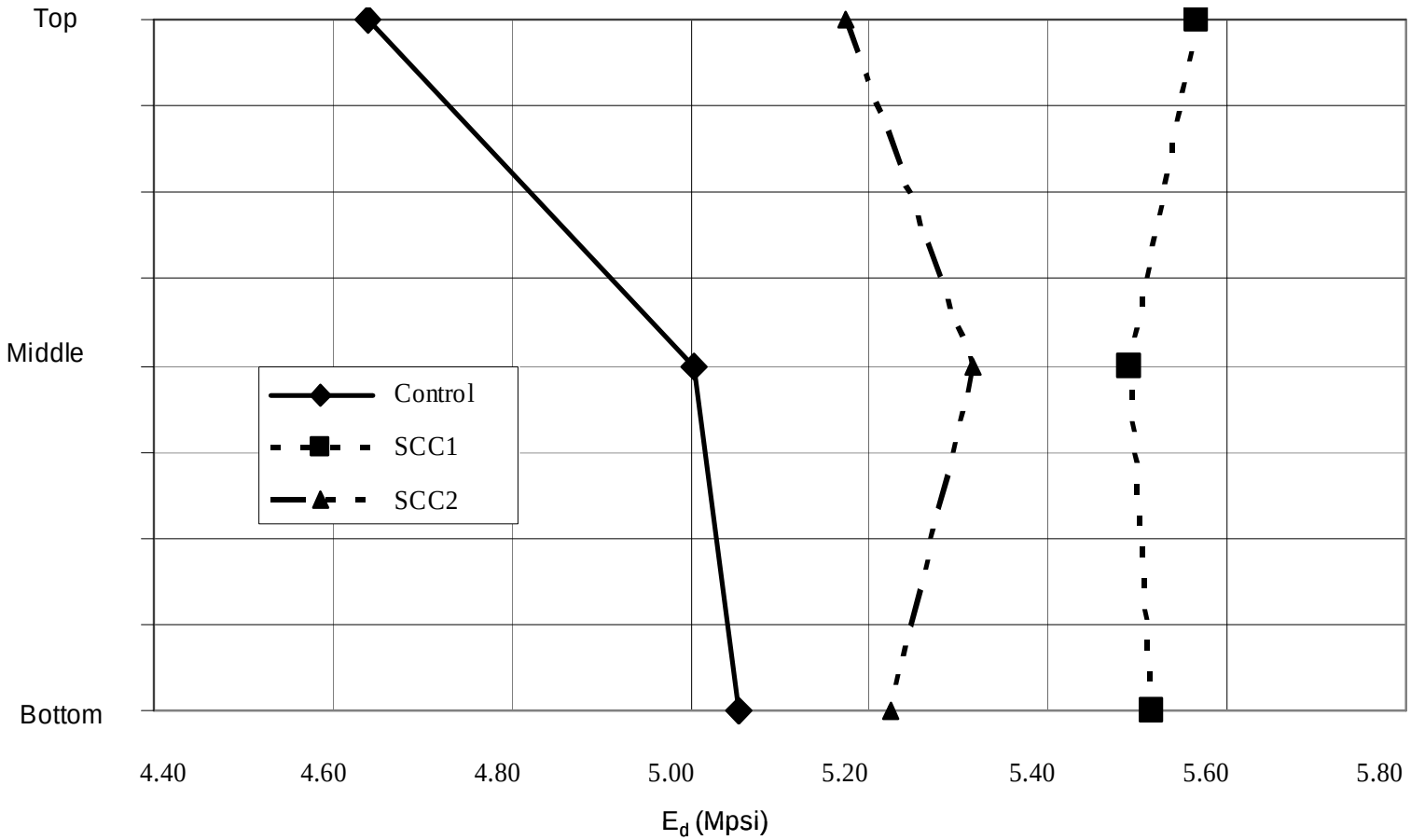

Figure 4.5 Dynamic modulus of elasticity at different depths using the average of two samples for each mixture

4.4.5 Air Permeability Index

The Air Permeability Index (API) average values for Control, SCC1 and SCC2 are summarized in Table 4.8. SCC1 and SCC2 had lower permeabilities. The API of the Control mixture is approximately twice that of the API from SCC1 and SCC2. API values for the Control mixture are comparable with values reported by Savas [2000] for similar conventional concrete mixtures after accelerated curing. There is no strong evidence of segregation in any of the mixtures but the values of API are relatively low and variation may be obscuring any trends.

4.4.6 Creep

Instantaneous elastic strain of the conventional concrete and SCC were measured as soon as the load was applied to the creep specimens at 90 days. The modulus of elasticity was calculated from the strain and the load for each creep frame. Results are shown in Table 4.2.

Figure 4.6 shows the creep strains of Control, SCC1 and SCC2 after loading at 90 days. Creep strain at 150 days was 134, 156 and 212 microstrain for Control C, SCC1 and SCC2, respectively. The specific creep can be calculated from equation 2.7 as:

For Control (per psi): $$r_u = \frac{134\times10^{-6}}{1870} = 0.072\times10^{-6}$$

For SCC1 (per psi): $$r_u = \frac{156\times10^{-6}}{2310} = 0.068\times10^{-6}$$

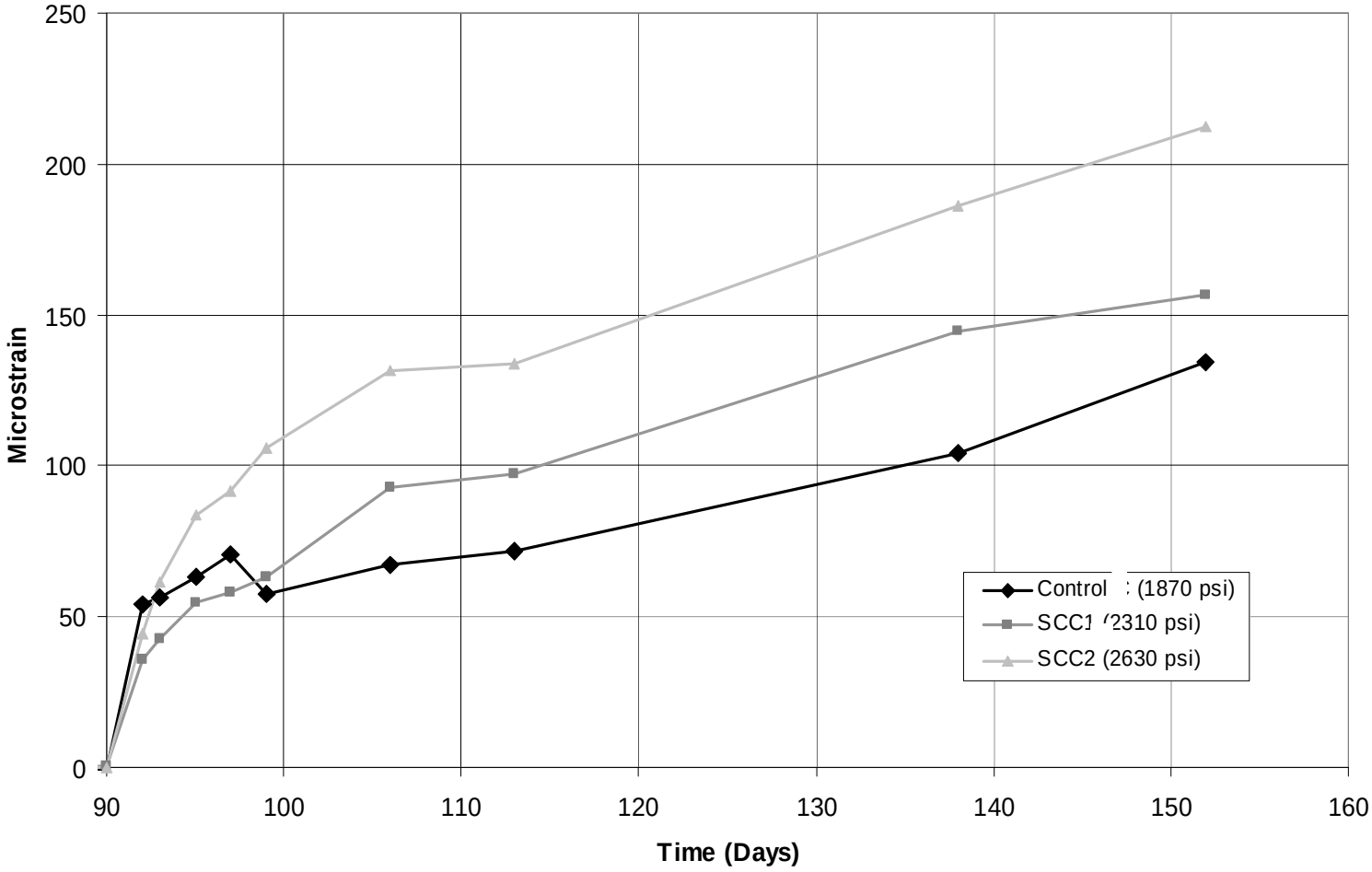

Figure 4.6 Creep strains of Control, SCC1 and SCC2 after loading at 90 days

For SCC2 (per psi): $$r_u = \frac{212\times10^{-6}}{2630} = 0.081\times10^{-6}$$

These values only represent a part of the creep response of each concrete since the load was applied at 90 days instead of at an early age of the concrete.

From Table 4.3, the prestressing force at the time of release was 512 kips after allowing 4% for loss due to elastic shortening and using a cross-sectional area of the girder of 560 in^2, the average prestress applied to the concrete can be obtained as:

$$f_i = -\frac{P_i}{A} = -\frac{512000}{560} = 914\,\text{psi}$$

and the average concrete elastic strain due to the prestress would be (Equation 2.1)

$$e = \frac{s}{E_{ci}} = \frac{914}{4.4\times10^{-6}} = 208\times10^{-6}$$

Using the creep coefficients given in Table 4.4, and from equation 2.8:

For Control $$e_{cr} = 2.76\times208\times10^{-6} = 574\times10^{-6}$$

For SCC1 $$e_{cr} = 4.00\times208\times10^{-6} = 832\times10^{-6}$$

For SCC2 $$e_{cr} = 7.00\times208\times10^{-6} = 1456\times10^{-6}$$

Specific creep can be obtained from Equation 2.12, using the average applied prestress in the concrete. Thus,

For Control $$r_u = \frac{574\times10^{-6}}{914} = 0.628\times10^{-6}\ \text{per psi.}$$

For SCC1 $$r_u = \frac{832\times10^{-6}}{914} = 0.910\times10^{-6}\ \text{per psi.}$$

For SCC2 $$r_u = \frac{1456 \times 10^{-6}}{914} = 1.593 \times 10^{-6} \text{ per psi.}$$

Specific creep values are summarized in Table 4.2. Since the load was applied at 90 days, these values represent the creep response of a mature concrete.

Creep can also be evaluated by using the increase in camber of the three girders studied between release and 90 days. As shown in Table 4.4, the initial camber was measured at the time of prestress released and later at 98 days. The creep coefficient can be obtained by dividing the camber at 90 days by the initial camber using the prestressing load and the elastic modulus as discussed in Chapter 2. The average growth of the camber for the two SCC girders was almost twice the camber growth of the control girder, which may be a cause of concern in terms of constructability.

Since considerable drying would have occurred by 90 days, the resultant creep strain may primarily be basic creep. The results of these tests indicate that the creep of SCC mixtures was slightly greater than 1.5 times that of control mixture, considering the variability of the data between SCC1 and SCC2. The results from the creep frame measurements also indicate a higher creep for the SCC mixtures. These findings imply that creep strain in the SCC concrete in a member would be considerably higher than that in a similar member produced using conventional concrete.

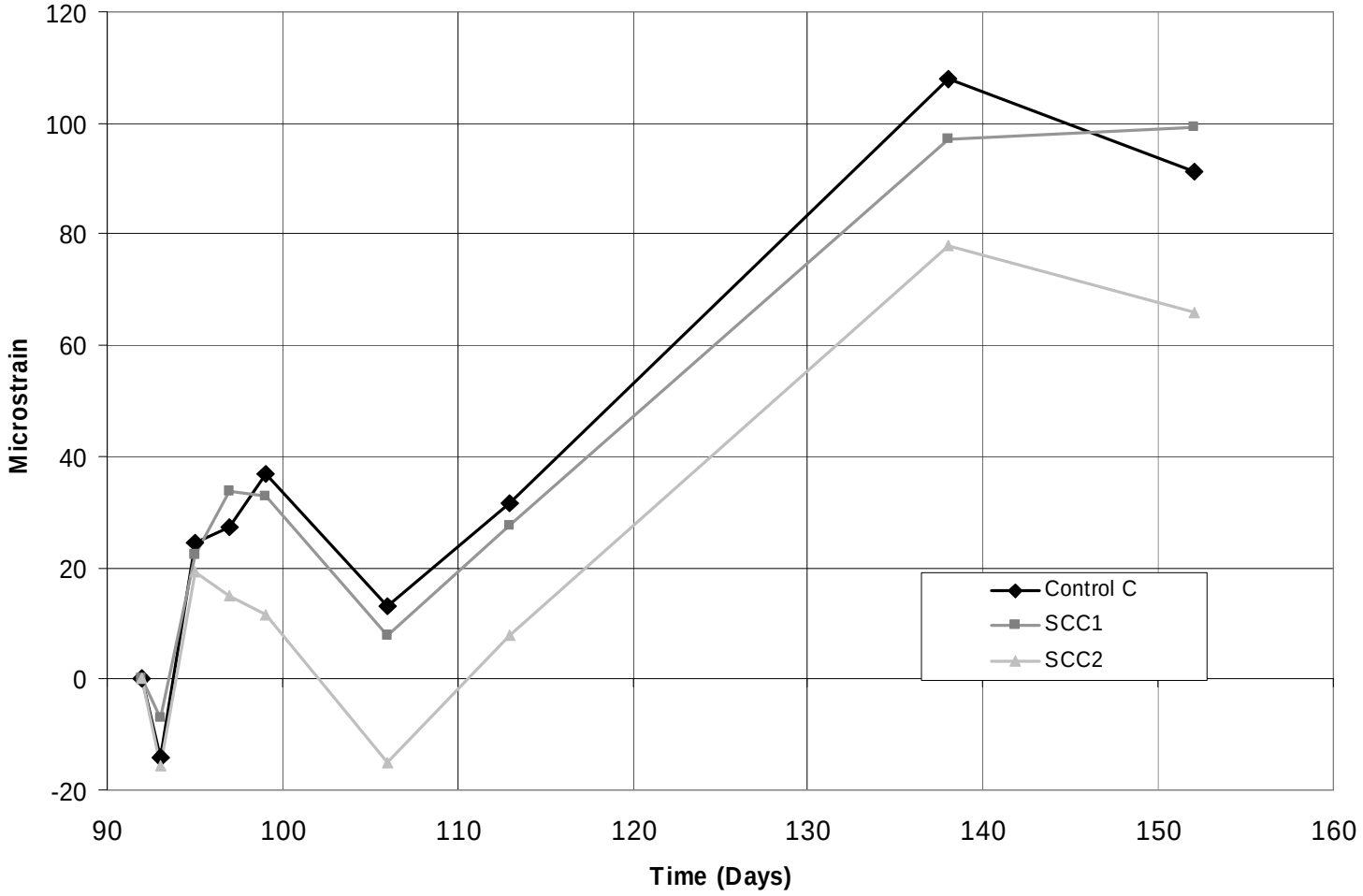

Figure 4.7 Shrinkage strains for Control C, SCC1 and SCC2 cylinder specimens

4.4.7 Shrinkage

Figure 4.7 shows the shrinkage strains of Control, SCC1 and SCC2 cylinders at 90 days. The conventional concrete shows a higher shrinkage than those of SCC1 and SCC2. As mentioned in Chapter 2, it was expected that the SCC mixtures would develop a higher shrinkage than conventional concrete due to the paste content. It is important to note that these values do not represent the total drying shrinkage of the specimens but shrinkage for a mature concrete.

Volume differences for Control and SCC2 mixtures are shown in Figure 4.8. An increase in volume was found. This is consistent with moisture uptake of a drier specimen exposed to a humid, external environment. Specimen drying is consistent with the lack of moist curing and the loss of moisture during the first 24 hours. The expansion is higher in Control than in SCC2. It appears, as expected, that SCC2 shows higher volume reduction, about 200 microstrain, in 105 days than Control, which showed little change (See Figure 4.9).

4.5 Girder Finishes

Surface finish, bugholes and the general appearance of the two SCC girders were similar to that of control girders, with no significant difference in the effort required for patching operations and finished product improvements. Surface finish after form removal are shown in Figures 4.10, 4.11 and 4.12 for Control, SCC1 and SCC2 girders respectively. Lower flowability than desirable may have affected the girder finish, obtaining

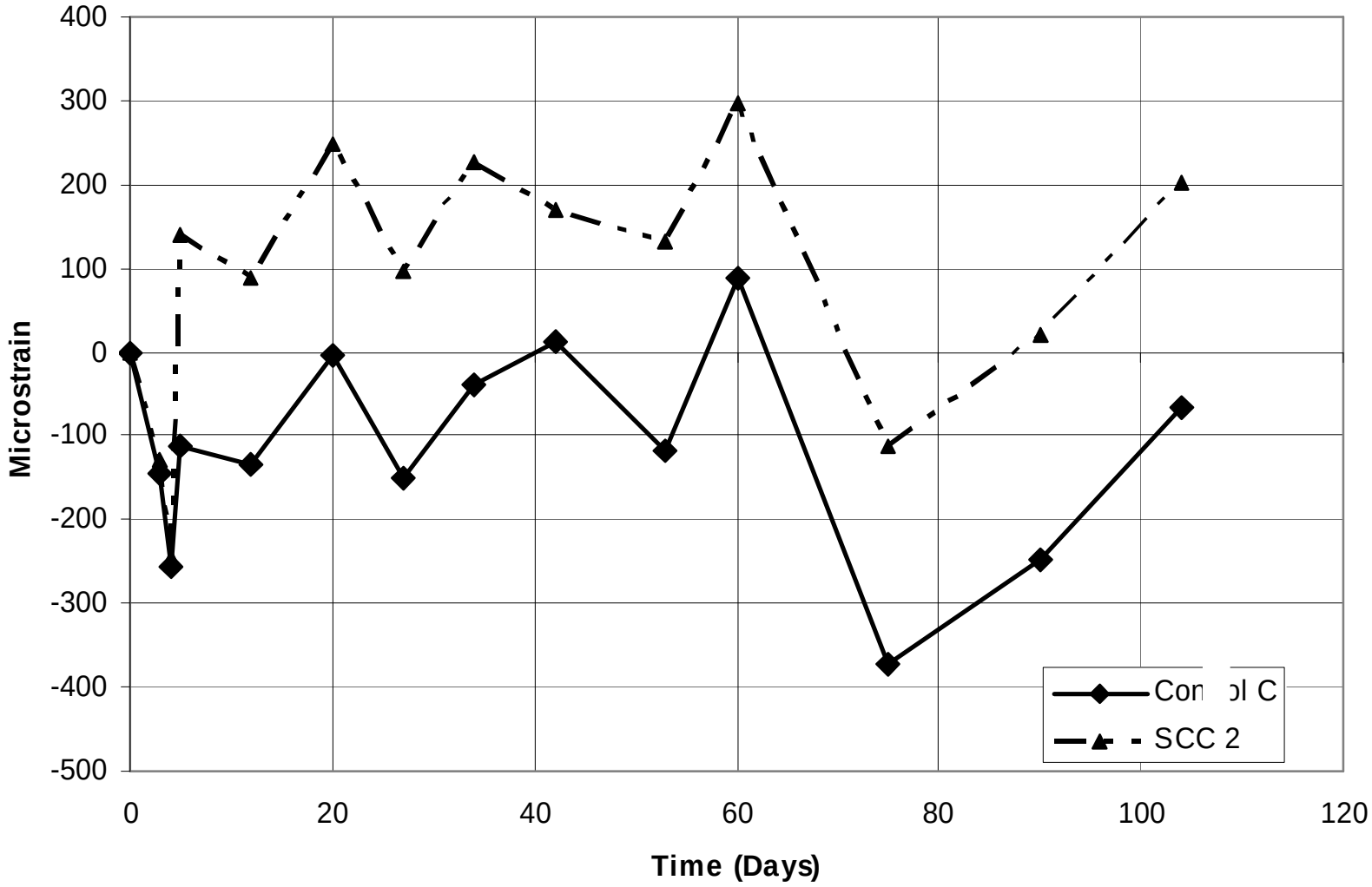

Figure 4.8 Shrinkage for Control and SCC2

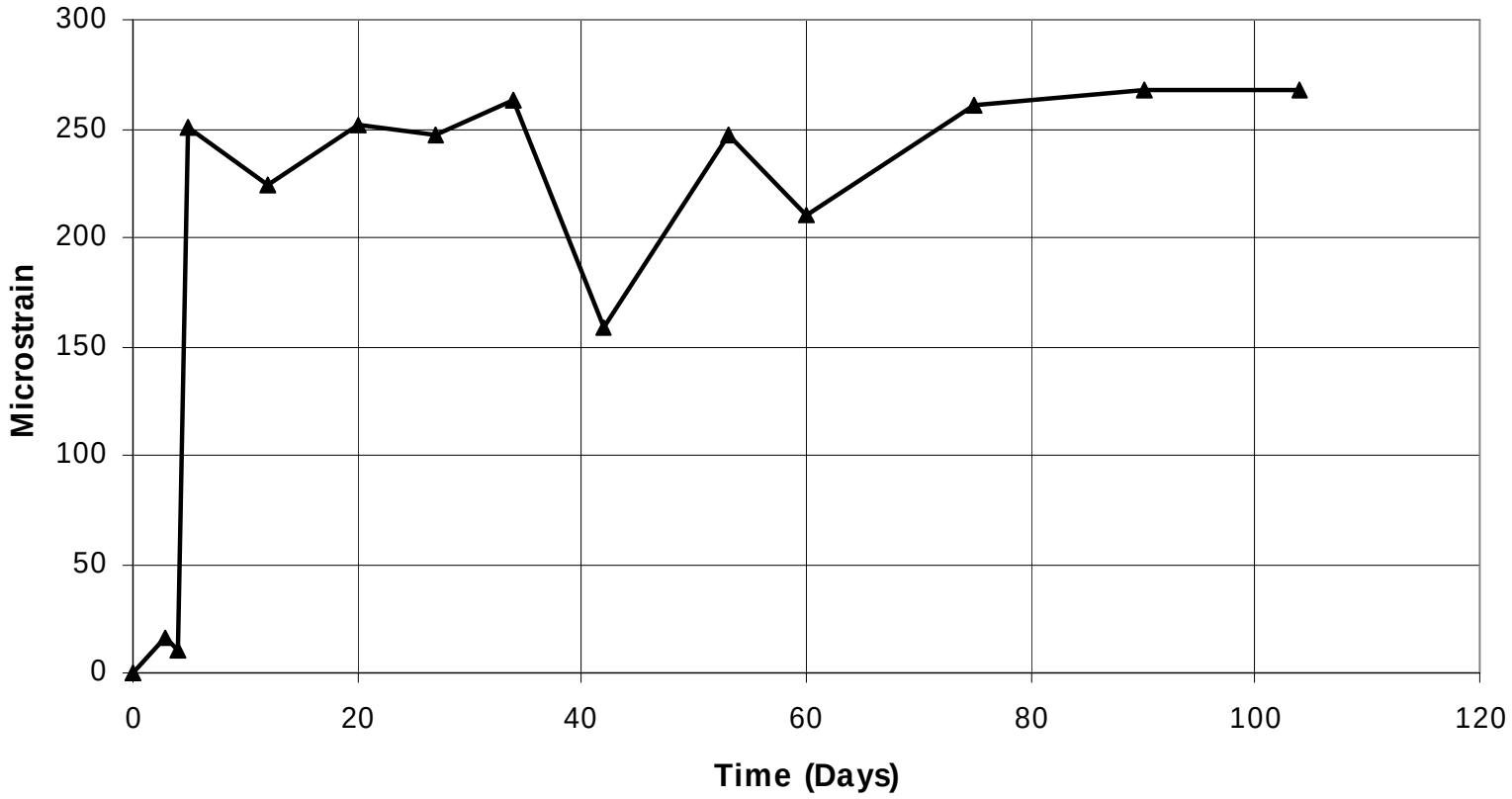

Figure 4.9 Difference in shrinkage between SCC2 and Control

Figure 4.10 Finish of Control girder

Figure 4.11 Finish of SCC1 girder

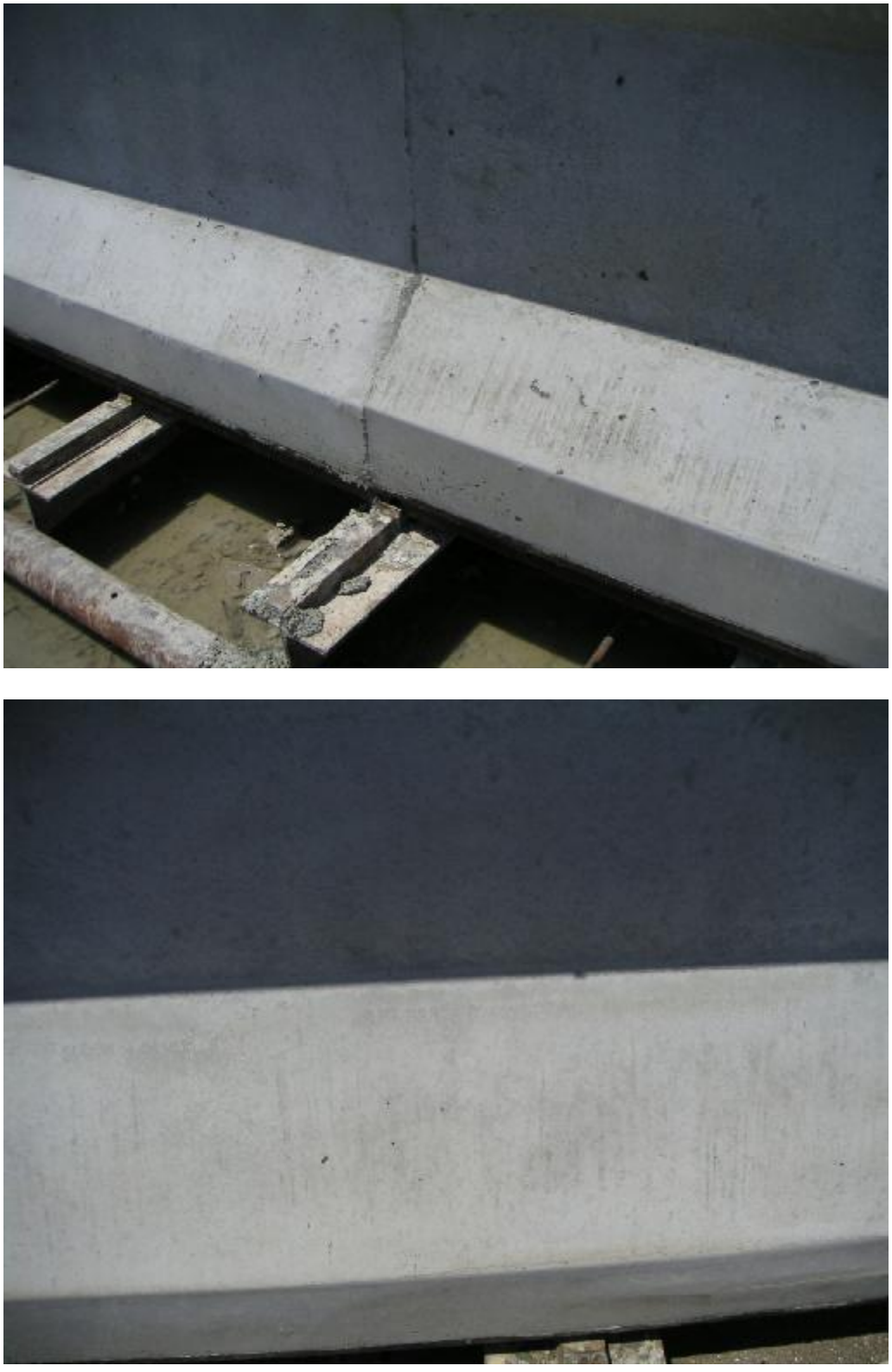

Figure 4.12 Finish of SCC2 girder

practically the same results as the girder cast with conventional concrete. The locations of areas with relatively large numbers of bugholes were similar in all girders. Practically no reduction in the labor cost would be obtained with these mixtures for finishing.

4.6 Load Testing of Girders

No cracks were observed after loading and full recovery of the girder deflection was found on unloading for all three girders. Figure 4.13 shows the plot for load-deflection for the three girders in this study. All the girders behaved elastically. The SCC1 was slightly stiffer than Control, while SCC2 was slightly less stiff than Control with no significant differences. The elastic modulus for each girder were obtained from the slope of the plot which are shown on Table 4.2.

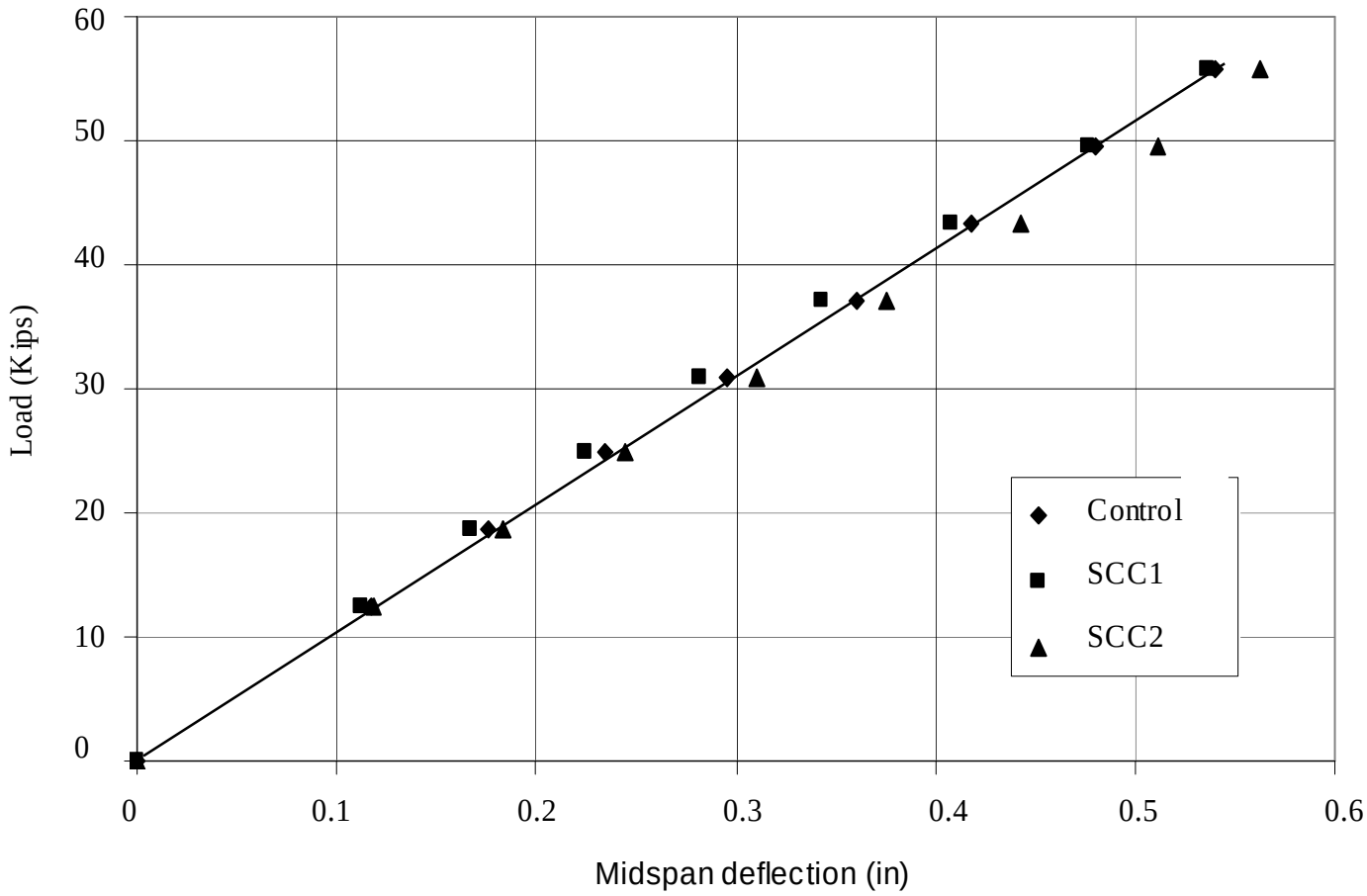

Figure 4.13 Load-deflection relationships of the three test girders

CHAPTER 5: CONCLUSIONS

Two AASTHO Type III girders were successfully cast without any vibration using SCC. The temperature recorded during the curing period for the two SCC girders and the conventional concrete girder were practically equal. Compressive strength of SCC at the time of release (18 hours) was higher than that of the conventional concrete and both exceed the required strength of 4,000 psi (27.6 Mpa). Compressive strength of SCC was also considerable higher than conventional concrete at all ages due to the higher cement content.

The flowability of the SCC did not reach the target value of 26 to 28 in (660 to 711) for either SCC1 and SCC2. The use of fly ash in the mixture may increase flowability, and affect the final cost of the mixture, however it will decrease the early strength of the concrete compared to using cement only. The use of fly ash may also increase costs due to installation of handling facilities.

No segregation was observed while testing the fresh SCC. Dynamic modulus obtained at different depth show no meaningful difference in mechanical properties between the top 1 inch and bottom 1 inch of 4x8 in test cylinders, therefore there was no evidence of segregation.

SCC1 and SCC2 had lower permeabilities than Control; the API of Control is approximately twice that of the API from the SCC mixtures. API values for the Control mixture are comparable with values reported by Savas [2000] for similar conventional

concrete mixtures after accelerated curing. These values are, however, reasonably close, indicating low permeability for all mixtures.

Comparison of elastic modulus between conventional concrete and SCC was complicated by the significant difference in strength. Examining the ratio of elastic modulus divided by square root of strength, the elastic modulus was approximately 15% lower for SCC than for conventional concrete at 90 days. Estimation of E_c using ACI equations for both conventional concrete and SCC was higher than measured values. The best model to predict E_c was that given by ACI 363, with a difference of 3.6% and 18.4% for conventional concrete and SCC respectively. A difference of 3% does not appear to be significant compared to the difference between predicted and measured E_c. Predicted E_c for SCC, however, shows at least a difference of 18%, which can be significant in the long term behavior of the girder.

The volume change of the shrinkage prism specimens showed cycles of shrinking and swelling for both conventional concrete and SCC, which followed the same trend over time. The difference between conventional concrete and SCC was approximately 210 microstrain during the testing period (105 days). Using the shrinkage data from comparison cylinder specimens measured during creep testing, the conventional concrete showed a higher shrinkage than those of SCC1 and SCC2.

The initial camber measured immediately after prestress release was practically the same for the three girders in the study. The load test results at 98 days showed that the modulus

of elasticity of the three girders did not increase appreciably in spite of the age difference of the concrete. The average growth of camber for the two SCC girders was almost twice the camber growth in the control girder. As expected, creep of the SCC was twice than that of regular concrete due to the higher paste and less coarse aggregate.

During the load test, the girders in this study behaved elastically and exhibited virtually identical load-deflection relationships up to the design service load, with no cracks observed. After unloading, all the girders exhibited full recovery of their deformations. These results indicate that the SCC girders are comparable to the conventional concrete girder and can be used as structural members.

LIST OF REFERENCES

Bartos, P. J. M., "An Appraisal of the Orimet Test as a Method for On-site Assesment of Fresh SCC Concrete", *International Workshop on Self-Compacting Concrete*, Japan 1998, pp. 403- 412.

Bui, V. K., Akkaya, Y., and Shah, S. P., "Rheological Model for Self-Consolidating Concrete," *ACI Materials Journal,* V. 99, No. 9, Nov –Dec, 2002, pp 549-559.

Campion, M.J., Jost, P., "Self-Compacting Concrete: Expanding the Possibilities of Concrete Design and Placement", *Concrete International*, April 200 pp 31-34.

Chan, Y.W., Chen, Y.S., Liu, Y.S., "Development of Bond Strength of Reinforcement Steel in Self- Consolidating Concrete", *ACI Materials Journal,* V. 100 No. 4, July – August, 2003, pp 490-498.

Dilek, U., Leming, M. and Guth, D., "Relationship Between Elastic Modulus and Permeability of Damaged Concrete," No.2471, Transportation Research Record, 2004 Transportation Research Board, Washington, DC.

Gerwick, B.C. Jr., Construction of Prestressed Concrete Structures, Second Edition, John Wiley and Sons Inc., 1993, pp 591.

Guth, D., Development and Evaluation of an Air Permeability Test Device for Concrete, Ph.D. thesis submitted to the Department of Civil Engineering, North Carolina State University, Raleigh, NC, December 1998, pp 230.

Interim Guidelines for the Use of Self-Consolidating Concrete in Precast/Prestressed Concrete Institute Member Plants, TR-6-03, Precast/Prestressed Concrete Institute, Chicago, IL, April 2003, 152 pp.

Kaszynska, M. and Nowak, A.S., "Effect of Mixing Tolerances on Performance of Self-Consolidating Concrete (SCC)," *Proceedings of the 3rd International Symposium on High Performance Concrete*, PCI, Orlando, FL, October 2003, CD ROM.

Khayat, K. H., and Guizani, Z., "Use of Viscosity-Modifying Admixture to Enhance Stability of Highly Fluid Concrete", *ACI Materials Journal,* V.94, No 4, July-Aug 1997, pp. 332-340.

Khayat, K.H., "Workability, Testing and Performance of Self Consolidated Concrete", *ACI Materials Journal*, V.96 No. 3, May-June, 1999, pp 346-352.

Khayat, K.H., "Optimization and Performance of Air-Entrained, Self-Consolidating Concrete," *ACI Materials Journal*, Sept-Oct 2000, pp 526-535.

Khayat, K.H., Assaad, J., "Air-void Stability in Self-Consolidating Concrete" ACI Materials Journal, V. 99, No. 4, Jul-Aug, 2002, pp 408-416.

Khayat, K.H., Assaad, J., Daczko J., "Comparison of Field-oriented Test Methods to Assess Dynamic Stability of Self-Consolidated Concrete," *ACI Materials Journal*, V. 101 No. 2, March –April, 2004, pp 168-176.

Lachemi, M., Hossain, K. M., Lambros, V., Bouzoubaâ., "Development of Cost-Effective Self-Consolidating Concrete Incorporating Fly Ash, Slag Cement, or Viscosity-Modifying Admixtures," *ACI Materials Journal*, V. 100, No. 5, Sept-Oct 2003, pp 419-425.

Leming, M. L., Nau, J.M. and Fukuda, J., "Non-destructive Determination of the Dynamic Modulus of Concrete Disks," *ACI Materials Journal*, Vol. 96 No. 3, May-June, 1999, pp. 391-396.

Martin, D. J., "Economic Impact of SCC in precast applications", *First North American Conference on the Design and Use of Self-Consolidating Concrete*, Center for Advanced Cement-Based Materials, Northwestern University, Nov 2002, Evanston, IL, USA, pp 147-153.

Means, M., PE, president S&G Prestress, Wilmington, North Carolina, private Conversation 2004.

Mehta, P. K. and Monteiro, P. J. M., Concrete: Structure, Properties and Materials, Second Edition, Prentice Hall, 1993, 548 pp.

Nawy, E. G., Prestressed Concrete: A Fundamental Approach, Fourth Edition, Prentice Hall, 2003, 939 pp.

Neville, A.M., Properties of Concrete, Fourth Edition, Jon Wiley and Sons, Inc., 1998, 844 pp.

Ouchi, M., Nakamura, S., Osterson, T., Hallberg, S., Lwin, M., "Applications of Self-Compacting Concrete in Japan, Europe and the United States," ISHPC, 2003 p 2-5.

Ozawa, K.,K. Maekawa, H. Kunishima, and H. Okamura, "Performance of Concrete Based on the Durability Design of Concrete Structures;" *Proceedings of the Second East-Asia-Pacific Conference on Structural Engineering and Construction*, Vol. 11,1989, p 445-456.

Ozawa, K., Maekawa, K., Okamura, H., "Self-Compacting High Performance Concrete", *Collected papers* (University of Tokio: Department of Civil Engineering), V. 34, 1996, p.135-149.

Okamura, H., "Self-Compacting High-Performance Concrete" *Concrete International*, July 1997, pp 50-54.

Okamura, H. and Ozawa, K., "Self-Compactable High Performance Concrete in Japan," International Workshop on High Performance Concrete, SP 169, American Concrete Institute, Farmington Hills, MI, 1994, pp 31-44.

Ozyldirim, C., Lane, S. Final Report: Evaluation of Self-Consolidating Concrete, Virginia Transportation Research Council, Charlottesville, Virginia, June 2003, VTRC 03-R13, 18 pp. (http://www.virginiadot.org/vtrc/main/online_reports/pdf/03-r13.pdf).

PCI Design Handbook, Precast and Prestressed Concrete, Fifth Edition, 1999.

Raghavan, K. P., Sarma, B. S., and Chattopadhyay, D., "Creep, Shrinkage and Chloride Permeability Properties of Self-Consolidating Concrete", *First North American Conference on the Design and Use of Self-Consolidating Concrete*, Center for Advanced Cement-Based Materials, Northwestern University, Nov 2002, Evanston, IL, USA, pp 301-306.

Savas, B. Z., Effects of Microstructure on Durability of Concrete, Ph.D. thesis submitted to the Department of Civil Engineering, North Carolina State University, Raleigh, NC, 2000, 190 pp

Schlagbaum, T., "Economic Impact of Self-consolidating Concrete (SCC) in Ready Mixed Concrete", *First North American Conference on the Design and Use of Self-Consolidating Concrete,* Center for Advanced Cement-Based Materials, Northwestern University, Nov 2002, Evanston, IL, USA, pp 131-136.

Skarendhahl, A., "Self-compacting Concrete in Sweden. Research and Application," *Proceedings of the International Workshop on Self-Compacting Concrete"*, Self-Compacting Concrete Sub-Committee, Concrete Committee. Japan Society of Civil Engineers, Tokyo, Japan, March 1999, pp 68.

Scholin, K. and Hilsdorf, H., " Permeability as a Measure of Potential Durability of Concrete Development of a Suitable Test Apparatus," Permeability of Concrete, SP 108, American concrete Institute, Detroit, MI, 1998 pp. 99-115.

Sonebi, M., Tamini, A., and Bartos., P.J.M., "Performance and Cracking Behavior of Reinforced Beams Cast with Self-Consolidating Concrete," *ACI Materials Journal*, V.100, No 6, Nov-Dec 2003, pp. 492-500.

Turcry, P., Loukili, A., Haidar, K., "Mechanical Properties, Plastic Shrinkage and Free Deformations of Self-Consolidating Concrete" *First North American Conference on the Design and Use of Self-Consolidating Concrete,* Center for Advanced Cement-Based Materials, Northwestern University, Nov 2002, Evanston, IL, USA, pp 301-306

Vachon, M., "ASTM Puts Self-Consolidating Concrete to Test", ASTM Standardization News, July 2002, pp. 34-37

APPENDICES

Appendix 1

Girder Properties

Girder Properties

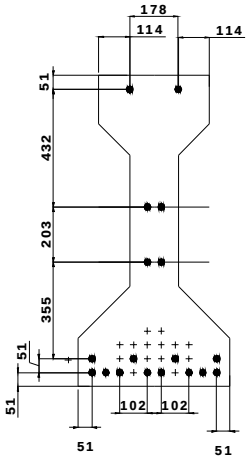

$A = 560\ in^2$

$Z_b = 6186\ in^3$

$I = 125{,}390\ in^4$

$Z_t = 5{,}070\ in^3$

$Y_b = 20.27\ in$

Wt = 583 #/ft

Specified f'_c at 28 days = 5,000 psi

Specified (18) ½ in L.R strands, all straight.

Eccentricity:

8 x 2 = 16

4 x 4 = 16

2 x 18 = 36

2 x 26 = 52

2 x 43 = 86

Total 18 206 $\qquad \frac{206}{18} = 11.44in$

$$e = y_b - 11.44 = 20.27 - 11.44 = 8.83in$$

Initial prestress for ½" strand = 33,000 per strand

At prestress transfer ½" strand = 31,000 per strand

Determine test load

Span = 16.7 m – 2x200 mm = 16.3 m = 53.5 ft

$$M_{DL} = \frac{583(53.5)^2}{8} = 208{,}586.5\, ft\#$$

$$f_{DL} = \frac{208{,}586.5(12)}{6186} = 404.6\, psi \text{ (T)}$$

P = 31,000 x 18 = 558,000

$$f = \frac{P}{A} + \frac{P_e}{Z_b} = \frac{558}{560} + \frac{558(8.83)}{6186} = 0.996 + 0.796 = 1.792 ksi = 1792\, psi \text{ (C)}$$

$$f = \frac{P}{A} + \frac{Pe}{Z_b} - f_{DL} = 1792 - 405 = 1387\, psi \text{ (C)}$$

If allowable tension in concrete is $3\sqrt{fc} = 3\sqrt{5{,}000} = 212$ psi

Applied moment required $= (1387 + 212)(Z_b)$

$= 1{,}599(6{,}186) = 9{,}891{,}414$ in#

$= 824.3$ ft k

$$\frac{PL}{4} = 824.3 \qquad P = \frac{824.3(4)}{53.5} = 61.6k \Rightarrow 30.8 \text{ Tons}$$

If not allowable tension used in design, then

Applied moment required $= (1387)(Z_b)$

$= 1387(6186) = 8{,}579{,}982$ in#

$= 715$ ft k

$$\frac{PL}{4} = 824.3 \qquad P = \frac{715(4)}{53.5} = 53.5k \Rightarrow 26.7 \text{ Tons}$$

Appendix 2 Compressive Strength at 7 days using 4x8 inches cylinder specimens

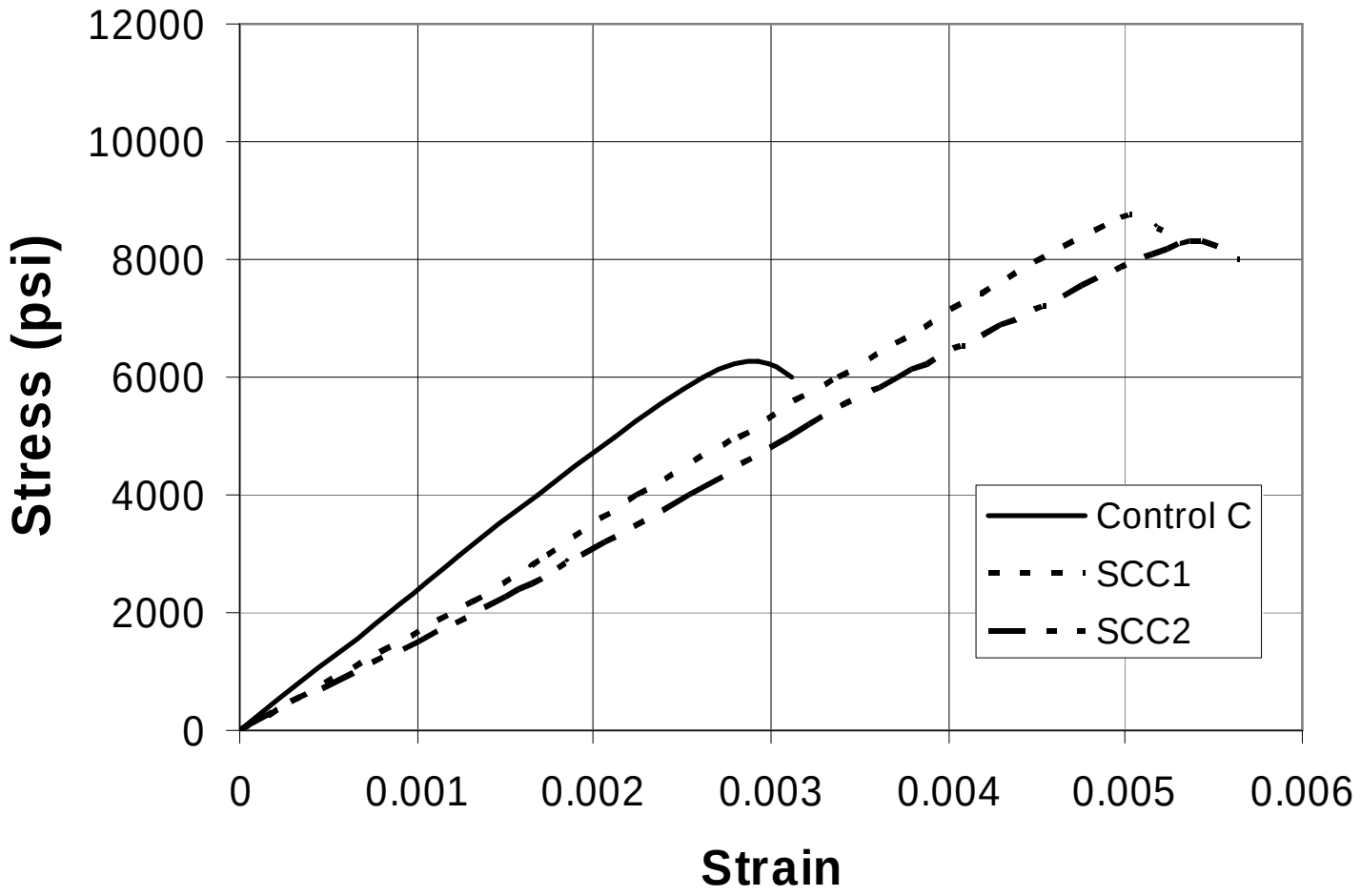

Appendix 2 Compressive Strength at 28 days using 4x8 inches cylinder specimens

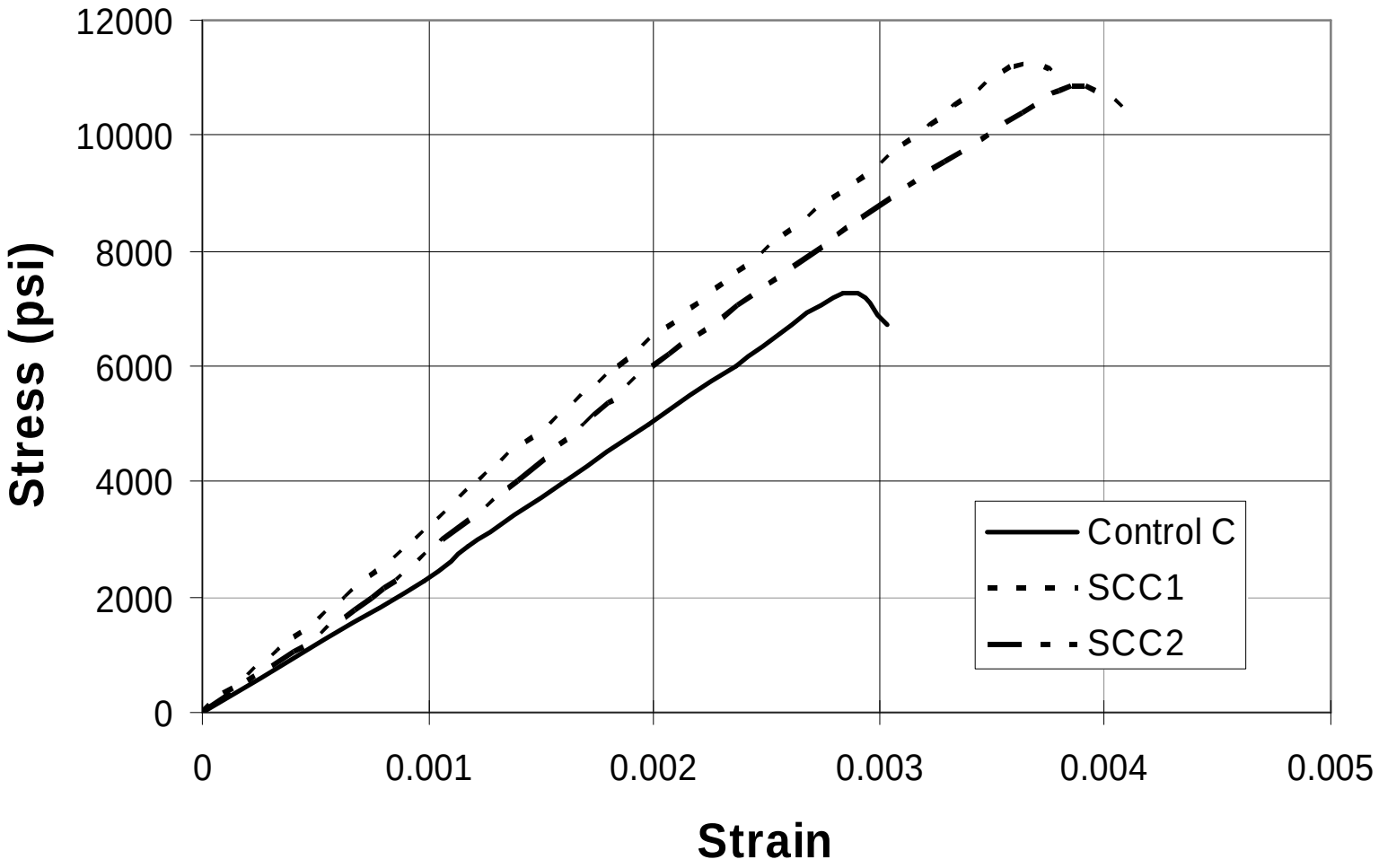

Appendix 4: Creep Data

Control C

													No Load					
				Control 7			Control 13			Control 16			Control 11			Control 15		
Date	**Time**	**Calibration**	**Conversion**	**A**	**B**	**C**	**A**	**B**	**C**	**A**	**B**	**C**	**A**	**B**	**C**	**A**	**B**	**C**
18-Aug		815		830	823	876	662	862	933	835	691	872						
Before Load		815	0.012877	831	824	876	662	863	933	835	691	873						
	90	815		831	824	876	662	863	933	835	692	873						
18-Aug		815		830	765	852	667	800	905	844	623	848						
After Load		815	0.012877	831	766	853	668	802	905	844	624	848						
	90.5	815		831	766	852	668	801	906	844	624	848						
20-Aug		815		829	760	850	667	792	903	841	622	844	836	902	945	846	841	913
		815	0.012877	829	760	850	666	792	903	841	621	844	835	902	945	845	841	913
	92	815		829	760	850	667	792	903	841	621	845	835	903	945	846	841	912
21-Aug		815		830	759	851	667	793	904	842	621	847	835	903	946	846	842	916
		815	0.012877	830	759	851	667	794	904	842	621	847	835	902	946	846	842	916
	93	815		830	759	851	666	793	904	842	621	847	835	903	946	846	841	916
23-Aug		815		829	755	848	665	789	901	840	618	844	832	901	944	844	840	912
		815	0.012877	829	755	848	665	788	900	840	619	843	832	901	944	844	840	911
	95	815		829	755	848	665	788	901	840	618	844	832	901	944	844	840	912
25-Aug		815		830	754	848	666	785	900	839	615	844	832	901	944	844	839	911
		815	0.012877	830	755	847	665	786	900	840	615	845	833	901	943	844	840	910
	97	815		830	755	848	665	785	901	840	614	845	833	902	943	844	840	911
27-Aug		815		830	754	848	666	786	900	841	616	844	831	900	942	844	839	911
		815	0.012877	830	754	849	666	785	899	841	616	844	832	900	942	844	839	912
	99	815		830	754	849	666	785	899	841	616	844	832	900	942	844	839	911
1-Sep		815		831	755	848	666	788	900	843	616	845	833	902	944	845	840	913
		815	0.012877	831	755	848	666	789	901	843	616	844	833	902	943	845	840	913

	106	815		831	755	848	666	788	901	843	616	844	834	902	944	845	840	913
8-Sep		815		830	754	846	666	784	900	843	613	842	833	901	942	844	839	912
		815	0.012877	830	754	847	665	784	900	843	613	843	832	900	942	844	839	912
	113	815		830	754	847	666	784	900	843	614	843	832	900	942	844	839	913
6-Oct		815		826	745	841	664	772	893	838	601	836	827	896	938	840	835	906
		815	0.012877	826	745	841	665	773	894	838	601	836	826	896	938	840	835	906
	138	815		826	745	841	664	772	893	839	601	836	826	895	938	840	835	906
20-Oct		815		829	741	840	666	768	893	842	597	834	827	897	938	841	836	909
		815	0.012877	830	741	841	666	769	893	841	596	834	827	897	938	841	836	909
	152	815		829	741	840	666	768	893	841	596	834	827	896	939	841	835	908

SCC1

													No Load					
				SCC1 20			SCC1 10			SCC1 17			SCC1 18			SCC1 19		
Date	**Time**	**Calibration**	**Conversion**	**A**	**B**	**C**	**A**	**B**	**C**	**A**	**B**	**C**	**A**	**B**	**C**	**A**	**B**	**C**
18-Aug		815		871	976	890	875	874	870	919	877	859						
Before Load		815	0.012877	871	976	891	875	874	872	918	878	860						
	90	815		871	976	890	875	875	871	918	878	860						
18-Aug		815		827	950	862	829	850	838	868	852	835						
After Load		815	0.012877	827	950	864	829	850	838	870	853	835						
	90.5	815		827	950	864	829	850	839	868	853	835						
20-Aug		815		823	947	863	825	848	839	865	851	834	850		869	943	778	1018
		815	0.012877	823	947	863	824	849	838	865	851	834	850		868	944	778	1018
	92	815		823	947	863	824	848	838	865	851	834	850		867	943	778	1018
21-Aug		815		824	947	863	824	848	838	866	850	833	849		868	945	779	1019
		815	0.012877	824	947	863	824	847	839	867	850	833	850		867	945	779	1019
	93	815		824	947	863	824	848	838	868	850	833	850		868	945	779	1019
23-Aug		815		821	946	860	820	848	834	863	849	829	849		868	941	776	1015
		815	0.012877	821	946	861	821	847	834	862	849	829	849		867	941	776	1016
	95	815		821	946	861	821	848	834	862	849	829	850		868	941	776	1015
25-Aug		815		820	945	861	820	845	835	860	847	829	849		864	941	776	1017
		815	0.012877	820	945	860	820	845	835	860	847	831	849		865	941	776	1017
	97	815		820	945	859	821	845	835	860	847	829	848		864	941	776	1017
27-Aug		815		820	945	859	819	845	835	861	846	829	848		866	941	776	1016
		815	0.012877	820	945	859	819	845	835	860	847	830	848		865	941	776	1016
	99	815		820	945	859	820	845	834	860	847	830	848		866	941	776	1017
1-Sep		815		819	946	859	819	845	835	858	846	830	849		867	943	778	1018
		815	0.012877	819	945	859	819	845	835	859	846	830	849		867	944	778	1018
	106	815		819	945	860	818	845	835	858	847	830	849		867	943	778	1018
8-Sep		815		818	944	859	816	843	833	856	846	828	847		866	943	776	1017

		815	0.012877	817	945	858	816	843	834	855	846	828	848		866	942	777	1017
	113	815		818	945	859	816	843	834	856	846	827	847		865	943	777	1017
6-Oct		815		808	936	853	807	836	827	848	838	822	843		861	939	772	1013
		815	0.012877	809	936	853	807	837	827	848	839	821	843		860	939	772	1013
	138	815		809	937	853	808	837	827	848	838	821	843		861	939	772	1013
20-Oct		815		808	936	852	805	836	827	844	839	821	843		861	939	772	1012
		815	0.012877	808	936	852	806	836	827	844	838	822	842		861	939	773	1012
	152	815		806	937	852	805	836	827	845	839	822	842		861	939	772	1013

SCC2

													No Load					
				SCC2 17			SCC2 8			SCC2 14			SCC2 10			SCC2 18		
Date	**Time**	**Calibration**	**Conversion**	**A**	**B**	**C**	**A**	**B**	**C**	**A**	**B**	**C**	**A**	**B**	**C**	**A**	**B**	**C**
18-Aug		815		880	845	839	871	843	873	829	872	860						
Before Load		815	0.012877	880	845	840	871	844	875	829	872	862						
	90	815		880	845	840	871	843	873	829	872	861						
18-Aug		815		835	815	807	823	813	846	780	844	833						
After Load		815	0.012877	835	815	807	823	813	846	780	844	835						
	90.5	815		835	816	808	823	815	846	780	844	835						
20-Aug		815		834	815	804	819	810	841	775	841	832	832	854	838	742	836	780
		815	0.012877	834	815	805	819	811	842	774	842	832	833	854	839	741	835	780
	92	815		834	815	804	819	811	843	775	842	832	832	854	838	742	836	780
21-Aug		815		833	815	805	818	810	844	775	840	832	834	855	840	742	835	780
		815	0.012877	833	815	805	819	810	844	775	840	832	834	856	841	743	835	780
	93	815		833	815	805	818	810	844	775	840	832	834	855	842	743	835	780
23-Aug		815		829	811	801	815	806	840	771	837	830	831	853	839	741	833	778
		815	0.012877	830	812	801	815	806	839	771	837	830	831	853	839	741	832	778
	95	815		829	811	801	815	806	839	771	837	830	831	853	839	741	833	778
25-Aug		815		829	811	800	813	806	840	770	837	829	832	853	839	742	833	778
		815	0.012877	829	811	800	813	807	842	770	837	830	832	853	839	741	833	778
	97	815		829	811	800	813	806	842	771	837	830	832	853	839	741	833	778
27-Aug		815		828	809	800	812	805	841	768	837	833	832	854	839	742	832	779
		815	0.012877	828	808	800	811	805	840	769	838	832	832	854	839	742	832	779
	99	815		828	809	800	811	805	840	769	838	831	832	854	839	742	832	778
1-Sep		815		829	809	800	812	805	841	769	837	830	833	856	841	743	834	780
		815	0.012877	829	808	800	812	805	841	769	837	831	833	856	841	743	834	780
	106	815		829	808	801	812	805	841	769	836	831	834	856	841	744	834	780

8-Sep		815		826	806	799	811	804	839	766	836	829	832	854	839	743	833	778
		815	0.012877	826	807	799	811	805	839	766	836	829	832	854	839	743	833	778
	113	815		827	807	800	811	805	839	766	835	829	832	854	839	743	833	778
6-Oct		815		817	800	790	802	798	832	758	829	820	827	850	835	738	828	774
		815	0.012877	817	800	791	802	798	832	759	829	821	827	850	835	738	828	774
	138	815		817	800	792	802	798	832	758	830	820	827	850	835	739	828	774
20-Oct		815		816	800	790	800	797	830	756	828	819	826	851	836	740	829	775
		815	0.012877	816	801	790	801	798	831	756	829	820	826	851	836	740	829	775
	152	815		816	801	790	801	797	832	756	829	820	826	851	836	740	829	775

Date	Time	Calibration		Control		SCC2	
				C-1	C-2	SCC2-1	SCC2-2
15-May	0	0.1932		0.3762	0.3729	0.2603	0.1151
		0.1935	0.1934	0.3762	0.3727	0.2602	0.1152
		0.1935		0.3762	0.3728	0.2602	0.1152
19-May	3	0.1907		0.3751	0.3717	0.2574	0.1156
		0.1908	0.1907	0.3753	0.3716	0.2572	0.1156
		0.1907		0.3752	0.3718	0.2573	0.1157
20-May	4	0.1927		0.3733	0.3775	0.2607	0.119
		0.1927	0.1927	0.3773	0.3773	0.2605	0.1192
		0.1927		0.3772	0.3775	0.2602	0.119
21-May	5	0.1967		0.3808	0.3771	0.2604	0.1185
		0.1965	0.1966	0.3808	0.3773	0.2605	0.1183
		0.1965		0.3806	0.3769	0.2601	0.118
28-May	12	0.1959		0.38	0.3769	0.2599	0.1184
		0.1958	0.1958	0.3801	0.3768	0.2598	0.1185
		0.1958		0.38	0.3769	0.2598	0.1184
4-Jun	20	0.1955		0.379	0.3741	0.2579	0.1161
		0.1955	0.1955	0.3791	0.3745	0.2577	0.1167
		0.1955		0.3789	0.3743	0.2577	0.116
11-Jun	27	0.1954		0.3793	0.377	0.2601	0.1169
		0.1952	0.1953	0.3792	0.3769	0.2602	0.1169
		0.1953		0.3793	0.3769	0.2601	0.1169
18-Jun	34	0.2043		0.3874	0.3842	0.2676	0.1249
		0.2043	0.2043	0.3876	0.3842	0.2675	0.1246
		0.2044		0.3876	0.3842	0.2674	0.1246
24-Jun	42	0.2008		0.3841	0.3796	0.2646	0.1218
		0.2009	0.2008	0.3837	0.3796	0.2645	0.1218
		0.2006		0.3839	0.3795	0.2646	0.1216
5-Jul	53	0.2019		0.3854	0.3831	0.2652	0.1244
		0.2014	0.2017	0.3854	0.3829	0.2648	0.1242
		0.2019		0.3854	0.3827	0.2647	0.1241
12-Jul	60	0.2002		0.3846	0.3763	0.265	0.1178
		0.2004	0.2003	0.3845	0.3764	0.2649	0.1176
		0.2004		0.3846	0.3763	0.2648	0.1176
19-Jul	67	0.1935		0.3735	0.3752	0.2528	0.1081
		0.1936	0.1935	0.3735	0.3752	0.2529	0.1081
		0.1935		0.3734	0.3752	0.253	0.1079
27-Aug	75	0.1815		0.3711	0.3672	0.2507	0.1082
		0.1851	0.1839	0.3712	0.3672	0.2506	0.1083
		0.185		0.3712	0.3671	0.2506	0.1082
8-Sep	90	0.1853		0.371	0.3675	0.2503	0.1085
		0.1854	0.1853	0.371	0.3674	0.2503	0.1085
		0.1853		0.371	0.3674	0.2503	0.1085
6-Oct	104	0.1853		0.3689	0.3654	0.2482	0.1066
		0.1854	0.1853	0.369	0.3654	0.248	0.1066
		0.1853		0.369	0.3654	0.2482	0.1066

20-Oct	118	0.1847		0.363	0.3598	0.2425	0.1061
		0.1847	0.1847	0.363	0.3599	0.2426	0.1062
		0.1847		0.3631	0.3599	0.2427	0.1061

Appendix 6: Concrete Disks data for Ed and API

	Disk samples from 1" cylinder molds								
	C-1	**C-2**	**C-3**	**SCC1-1**	**SCC1-2**	**SCC1-3**	**SCC2-1**	**SCC2-2**	**SCC2-3**
Dry weight (g)	483.18	536.38	495.95	534.75	565.18	444.24	508.12	513.95	525.53
Wet weight (g)	270.35	301.13	277.5	303.59	322.43	251	284.5	285.68	289.63
Diameter (in)	**4.007333**	**3.9955**	**4.00767**	**4.0155**	**4.012833**	**3.995333**	**3.995167**	**4.009333**	**3.9905**
Diameter (m)	**0.101786**	**0.101486**	**0.10179**	**0.101994**	**0.101926**	**0.101481**	**0.101477**	**0.101837**	**0.101359**
Area (m)	0.008137	0.008089	0.00814	0.00817	0.008159	0.008088	0.008088	0.008145	0.008069
Thickness (in)	1.067125	1.183125	1.098	1.151375	1.224	0.97625	1.11625	1.12825	1.17875
Thickness (m)	0.027105	0.030051	0.02789	0.029245	0.03109	0.024797	0.028353	0.028658	0.02994
Frequency	11647.67	12981.33	11827.3	13118	13186.67	11403.67	12467.33	12569.33	13108.67
Time (sec)	1878	1382	1150	2094	2660	2460	2450	3611	4126
API 1 (m2/s)	0.056984	0.086363	0.09573	0.054917	0.04602	0.040037	0.04597	0.031302	0.028892

	Disks sawn from 4 x 8 cylinders (Top, middle, bottom)								
	C-14 T	**C-14 M**	**C-14 B**	**C-18 T**	**C-18 M**	**C-18 B**	**SCC1-7 T**	**SCC1-7 M**	**SCC1-7 B**
Dry weight (g)	454.59	483.38	445.91	424.57	468.99	445.22	448.37	467.42	486.6
Wet weight (g)	254.66	275.76	254.84	238.8	266.23	254.95	258.62	267.92	276.81
Diameter (in)	**4.053333**	**4.0215**	**4.001**	**4.041333**	**4.0375**	**3.997333**	**3.998333**	**4.016167**	**4.045167**
Diameter (m)	**0.102955**	**0.102146**	**0.101625**	**0.10265**	**0.102553**	**0.101532**	**0.101558**	**0.102011**	**0.102747**
Area (m)	0.008325	0.008195	0.008111	0.008276	0.00826	0.008097	0.008101	0.008173	0.008291
Thickness (in)	0.94975	1.0135	0.928375	0.89	0.988625	0.935625	0.943875	0.964963	0.9895
Thickness (m)	0.024124	0.025743	0.023581	0.022606	0.025111	0.023765	0.023974	0.02451	0.025133
Frequency	10921.67	12028.67	11500	10793.67	11808.33	11555.33	12196.67	12218.67	12197.33
Time (sec)	1680	2562	2126	3364	4080	1920	7940	45647	12530
API 1 (m2/s)	0.055414	0.039393	0.043931	0.026087	0.023938	0.049114	0.011975	0.002111	0.007772

	Disks sawn from 4 x 8 cylinders (Top, middle, bottom)								
	SCC1-11 T	**SCC1-11 M**	**SCC1-11 B**	**SCC2-1 T**	**SCC2-1 M**	**SCC2-1 B**	**SCC2-3 T**	**SCC2-3 M**	**SCC2-3 B**
Dry weight (g)	463.85	543.61	501.32	464.59	467.76	471.11	500.3	472.73	454.51
Wet weight (g)	264.84	309.83	287.59	260.6	262.11	265.45	281.3	266.71	257.2
Diameter (in)	**4.0038333**	**4.0221667**	**4.0475**	**4.034333**	**4.0035**	**3.986833**	**4.056867**	**4.016667**	**3.9965**
Diameter (m)	**0.1016974**	**0.102163**	**0.1028065**	**0.102472**	**0.101689**	**0.101266**	**0.103044**	**0.102023**	**0.101511**
Area (m)	0.0081229	0.0081974	0.008301	0.008247	0.008122	0.008054	0.008339	0.008175	0.008093
Thickness (in)	0.97375	1.122375	1.0115	0.99075	0.9895	1.018	1.80525	1.01225	0.972
Thickness (m)	0.0247333	0.0285083	0.0256921	0.025165	0.025133	0.025857	0.045853	0.025711	0.024689
Frequency	12389	13400.667	12577.333	12211	12376	12608.67	12399.67	12569	12140.33
Time (sec)	6202	12994	3405	29768	22560	6406	3120	27600	14400
API 1 (m2/s)	0.0157728	0.0085985	0.0292025	0.003293	0.004407	0.016101	0.056617	0.003661	0.006806